We thank all reviewers for their constructive comments, which helped to improve the paper. Below, we address all comments point-by-point.

#reviewer1

This paper describes the XCO2 retrieval from OCO-2 spectra with the RemoTeC algorithm for two years of data, focused on TCCON collocations for validation purposes. OCO-2 currently delivers the most accurate and the largest dataset of NIR / SWIR radiance measurements for XCO2 estimation. RemoTeC is widely acknowledged as a state-of-the-art retrieval algorithm, already successfully applied to GOSAT. The retrieval of OCO-2 with RemoTeC is therefore widely expected and this work largely deserves a dedicated publication. The paper is well written and concise. The main properties of OCO-2 are clearly reminded. The main assumptions of RemoTeC are recalled, but I understand that a detailed description of the algorithm requires to read references, which may be a weakness for the self consistency of the paper. Maybe the paper should be more precise about the modification of the algorithm for OCO-2. The methodology is based on the systematic comparison with several TCCON stations. This is a classical, rigorous and probably the most accurate strategy for XCO2 missions, as the column sensitivities are similar and strong efforts have been made to trace the TCCON network to the WMO XCO2 standard. Such validation work requires estimation of random error, global and regional biases, which can only be obtained at a reasonable cost with the large data set of the TCCON network. The choice of a period larger than 1 year is essential to remove the seasonal effects.

The main result is that the residuals biases of OCO-2 / RemoTeC with the TCCON global network is lower than 0.1 ppm in absolute value, and up to 1 ppm when looking at individual stations. These low values, of the same order as the OCO-2 L2, prove the quality of RemoTeC and its application to OCO-2. The remaining station to station biases are still high for the needs of the flux community, meaning that research must continue to improve the retrieval scheme and the understanding of the instrument (beyond the scope of this paper). The bias correction shows its efficiency to empirically reduce the biases, but the magnitude of the correction is still too high to give a solid confidence in the final value.

I have some questions and remarks that I would like the authors to address before publication. These will probably not require new calculations, but only precisions and additional materials. I will try to focus my questions on the application of RemoTeC to OCO-2 and not to the RemoTeC algorithm itself which was the subject of previous papers properly quoted. (1)-One of the drawbacks of this paper is that literature on this topic is large, and the reasons of some assumptions have now become implicit (and could sometimes deserve to be questioned once again). (2)-I also noticed that several results are given only in the text whereas they show be given dedicated figures or tables (see comments). This has to be corrected before publication. (3)-Finally, I was sometimes lost in the different statistics indicator (target, land, ocean; all footprints or daily averages; global bias, station to station bias, standard deviation). A clearer presentation and interpretation of them would be welcome before publication.

C1-Page 3 line 13: The objective of the study requires further justification than « to enhance the reliability and confidence of the data product ». What does this study aim at? To challenge the official OCO-2 Level 2 (L2)? To improve RemoTeC through its application to the new OCO-2 dataset, more accurate than GOSAT? Will a new OCO-2 / RemoTeC be proposed in the future?

R1-. We added a phrase " We expect that application of RemoTeC to OCO-2 data will lead to a better understanding to the capabilities and limitations of the OCO-2 instrument and the operational level-2 data product. Furthermore, we see this work as a first step towards processing a larger data set with RemoTeC." For example, in this paper we show that RemoTeC the bias correction only has a minor effect on the XCO2 retrieval accuracy, while for the official level-2 product a much larger correction is needed. This suggests that the need for bias correction is for large part caused by the algorithm itself rather than by instrument related errors. Also we show that it is needed to fit an intensity offset which gives insight into instrumental errors of the OCO-2 instrument.

C2-As already mentioned, there is a lack of description of the algorithm, largely given by references. This is however very important to understand the differences with the OCO-2 L2.

R2- One major modification on RemoTeC/OCO-2 is that now we adopted a vector radiative transfer model (LINTRAN V2) to the retrieval scheme. Scattering is considered for ocean glint retrievals. Before, in GOSAT application, RemoTeC uses a scalar radiative transfer model for land and performs non-scattering retrieval for ocean glint. We add " For OCO-2 application, several modifications have been made to the algorithm: (1) a vector radiative transfer model (LINTRAN V2) is employed in the retrieval scheme; (2) Aerosol scattering effects are taken into account for ocean glint retrievals; (3) Information on pressure profiles, humidity and temperature are extracted from the ECMWF data with a resolution of 0.125 by 0.125 instead of 0.75 by 0.75 previously. ".

C3- p4 l12: 5° around a TCCON station is very large (~500km). In such an area the CO2 may not be considered as uniform. What is your justification? Did you make any error budget, any sensitivity study?

R3- The CO2 may be inhomogeneous in this area. However, in the validation we do not see a clear dependency between XCO_2 difference and the collocation distance, as shown in Figure 1. We add "Here, the dependency of difference with collocation distance and surface pressure is negligible. " in section 4.1 in the paper.

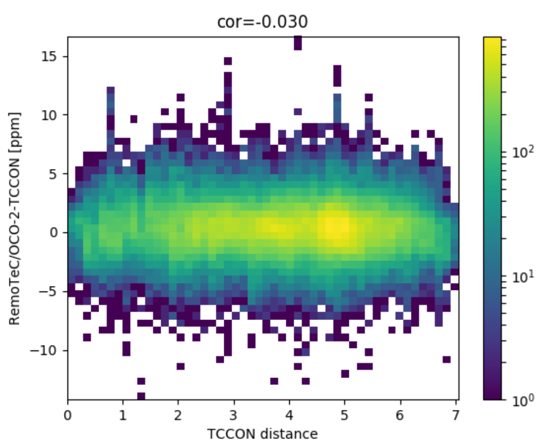

Figure 1. Dependency between XCO_2 difference and TCCON distance (unit degree).

C4-p4 l16: Why do you restrict VZA to <30° and not to a larger value? Is there also a restriction on SZA? Table 1 gives some information but in contradiction for VZA, maybe because it only applies to land and glint? Please precise.

R4- Here, we select a subset of Target data by restricting VZA<30° only for computational reasons. We do this only for target data because the amount of data becomes too large otherwise. Current retrieved target data already include more than 200.000 soundings (before quality filtering). The restriction on SZA (<70°) is listed in Table 1. We add a phrase " This viewing zenith angle restriction has only been applied for target observations for time efficiency".

C5-- p5 & 6: I think the paper deserves a table describing exactly the content of the state vector.
R5- Thanks for the suggestion. Table 1 is added to describe elements of the full state vector.

C6-p6 l13: the description of the cloud screening is too light, I understand it is a copy of what is done by OCO-2. Do you use the information from the OCO-2 pre-processing, or did you develop your own algorithm? Did you make any performance study, and associated XCO2 sensitivity study? 30% is higher than the performance reached by OCO-2 (for land and ocean).
R6- It is not a copy of OCO-2 cloud filtering. We use our own no-scattering retrieval algorithm. We also do not use OCO-2 pre-processing and we use a pre-processing algorithm developed at SRON. We modified in the paper " For this purpose, we implemented a fast non-scattering retrieval as part of the RemoTeC and…….. Cloud filtering are performed by applying following criteria: 0.885<O2_ret/O2_ecmwf<1.020, 0.990< CO2_swir1/CO2_swir2 <1.035 and 0.950<H2O_swir1/H2O_swir2<1.060…….For target, land and ocean glint observations, the percentage of clear soundings are 24%, 28% and 34%, respectively. For now, we mainly use those ratios as a option to filter cloud contaminated cases in the retrieval. "

C7-p6 l28: please explain the reason why you separate land and ocean evaluation. Is it based only the aerosol argument (p7 l19)? Was it decided from the OCO-2 feedback ? OCO-2 does also but with another separation between land nadir and land glint.
R7- Land and ocean evaluations are separated because they have very different sensitivity to aerosols. In contrast, we found that land nadir and land glint are very similar in terms of performance against TCCON so in our opinion there was no need to separate the two.. We now add "The separation is due to the fact that land and ocean surface reflections are modeled differently".

C8-p6 l33: the assumption that TCCON station to station variability is zero is very strong and may not be excluded when interpreting the results.
R8-Yes, that's true. We emphasize this "However, as discussed by Kulawik et al. (2016); Buchwitz et al. (2017b), individual stations have a year-to-year variability of ~ 0.3 ppm and the overall TCCON XCO2 uncertainty is around 0.4 ppm (1-sigma).".

C9-p7 l8: you talk about retrieval uncertainties; these uncertainties may be instrument dependent. Compared to Butz et al 2011, Gueret et al 2013b, did you reconsider your filters for OCO-2?
R9-Yes, the filters are reconsidered. For example. The range of aerosol parameters are filtered differently compared with that used for GOSAT retrievals[ref1]. Moreover, some specific filters for OCO-2 are used such as intensity-offset ratios in SWIR1 and SWIR2 channels.

C10-p7 l25: I don't understand why you say « we look for possible correlations of errors with instrumental, geophysical, meteorological and retrieved parameters ». Actually, here you do not look for such correlations (as would the OCO-2 Bias Correction do), you only calculate a regression with chi2, which is different. This is an original bias correction and, as far as I know, it is the first time it is applied. What made you adopt such methodology? To my mind its drawbacks are that you loose interesting spectral information about the residuals. An error in retrieved albedo may lead to a large chi2 whereas it has very limited impact on XCO2. An error in line-mixing may lead to a small chi2 residual but have a strong impact on XCO2. I clearly do not say the approach is wrong, but I think that it is new and should really deserve deep study. The shape of the chi2 spectra would deserve attempts of interpretation. Why would you have only to regress with chi2 in SWIR-1 and not in the other bands? Why would this bias correction be required only for land, not for oceans? The spectroscopy and the instrument are the same. You say in section 4.1 the aerosol contribution is weak in ocean glint measurement, that could be an explanation but aerosols are not the only source of bias.

R10- We checked the correlation between the parameters mentioned here and we see relatively high correlation with chi2. In the 'Supporting Information' (SI) (**Figure s1**), we include the correlation plots with six parameters: air mass, water column, blended albedo, mean signal in O2 A-band, aerosol ratio and aerosol size parameter. We only do the regression with chi2 in SWIR1 (similar performance can be achieved by using chi2 in the SWIR2 band) simply because it gives the best validation results after bias correction (although it should be mentioned that the overall effect is small). We also tried other parameters like surface albedos, mean signal in O2A band, water column and overall fit residual to do the bias correction, but the station-to-station bias becomes somewhat worse. The correlation with chi2 tells us that the XCO2 error (before bias correction) increases when the forward model is less capable in fitting the measurements or if the pure instrumental noise becomes small (and the chi2 large if the fit residuals stay the same) .The latter effect may happen over bright surfaces where it is more difficult to account for aerosol scattering.. The main effect of the bias correction over land is reducing the overall mean bias. For ocean, we directly subtract a mean bias. For sure, aerosols are not the only source of bias, but I think it is still outstanding among possible bias sources in our retrieval.

C11-p22: figure 4 should exhibit a fit, be given for lands and oceans, and for the 3 spectral bands.
R11- A linear fit is included in Figure 4. For ocean, these parameters are not used in the bias correction and we only subtract an overall mean bias. The term fit residual was incorrectly chosen and hence we changed it to chi2.

C12-p8 l9: you say some correlation with parameters of table 1 are reduced, you clearly have to present these correlations by a figure or table before and after bias correction. Otherwise we cannot accept such affirmation.
R12-We add **Table s1** in the 'Supporting Information' (SI) section to list correlations between parameters of Table 1, before and after bias correction.

C13-p8 l19: please show fig 2 before and after bias correction. Giving a rough value in the text (~0.1ppm) is not enough.
R13- The results before bias correction are shown in SI **Figure s3**.

C14-p8 l23: please define your averaging. I understand that in fig 2 (no averaging), you plot every OCO-2 single footprint minus the TCCON of the area at the same time. I understand that in fig 5, 6, 7 you average every OCO-2 single footprint – TCCON at the same in a window 5°*5°*2h, is that true? Is it mean(OCO-2) – mean(TCCON)? You mention a « daily averaging » p8 l32, but this term is confusing because you may encounter several collocations with several TCCON during the same day. In such a case, are the data of different TCCON in the same average? If not, you should maybe talk about « overpass averaging »?
R14-Indeed, we are actually doing overpass averaging and compare mean(OCO-2) with mean(TCCON). We modify this through the paper.

C15- p8 l23: Please explain why you make an averaging in 4.2 whereas you do not in 4.1. I guess that in 4.1 you need to keep the individual parameters for your bias correction derivation, but this clearly needs to be explained. For this reason, fig 2 and fig 5,6,7 cannot be directly compared, and that is why the effect of bias correction is difficult to assess.
-p9 l1 and fig 5,6,7: Please also give the figures before bias correction for fig 5,6,7, and give the

associated standard deviation as for p8 l33.

R15- To give a better view on the effects of bias correction, we include overpass averaging figures before bias correction in the attachment (**Figures s4,s5,s6**). We add sentences to explain why we use individual retrievals in the bias correction "When comparing individual retrieval results with collocated TCCON measurements, we look for possible corrections of errors with instrumental, geophysical, meteorological and retrieved parameters. This correction should be valid for each single sounding and thus evaluated with individual results."

C16- p9 l10: please illustrate the effect of bias correction by giving figure 8 also for before bias correction.
- p9: I know you made the assumption the TCCON stations are consistent (p6 l34), but I am disappointed that you do not try to interpret the station to station variability in terms of residual bias of OCO-2 / RemoTeC or actual differences between TCCON stations. The fact that you do not see the same station to station bias in land and oceans modes could suggest there are still biases in OCO-2 /RemoTeC.

R16- We now include results before bias correction as that of Fig. 8, Fig.9 and Fig.10 in attachment (**Figure s7, s8, S9**). The station to station bias in land and ocean retrievals are close to each other(0.41 ppm vs 0.44 ppm) but it is important to note that these values are derived from different (number of) stations.

C17- p10 l6: Did you try also the same retrieval as fig 6 without the fit of the offset in the O2 band? As you mention later, there could be a link with the stronger internal reflections in this band.

R17-No, for now this retrieval setting (without the fit of the offset in the O2 band) has not been tested.

C18- p10 l12: I am not convinced by the explanation of the lack of SIF fitting, since the behaviour of the SIF and the offset is very different (SIF exhibits atmospheric absorptions).

C18-We deleted this phrase.

C19- p10 section 5: I think the comparison with the previous OCO-2 / ACOS – TCCON and with the previous GOSAT / RemoTeC – TCCON are very important. But here the discussion is poor, mentioning only the common results in terms of standard deviation. This section really deserves to compare biases (global, station to station, etc.), as it was the case for section 4. This could help understand the origin of biases (from TCCON, from the instrument, the retrieval code). This should be done before and after bias correction.

C19- We added a paragraph in section 5 that directly compares ACOS and RemoTeC before and after bias correction for common data points.

C20- p2 l9: for clarity I would make a new paragraph.

R20-modified

C21- p4 l3: please precise if you use the tabulated instrumental functions given in the OCO-2 products.

R21-modified

C22- p4 l12: you use a requirement in degrees rather than in km, why? This makes a distance criterion in km variable according to the station, which is not suitable.

R22-As can be seen above in Figure.1, there is no clear dependency between XCO2 difference and distance under current collocation criteria.

C23- p4 l18: please precise is you make your own calculation of surface pressure from ECMWF and MNT (this information could also be read from the OCO-2 L2 data). How do you interpolate ECMWF and how to select SRTM grid points? This question makes sense since you do not retrieve surface pressure in your state vector.

R23- The interpolation is performed with linear interpolation in time and nearest neighbor in space. All SRTM grid points within certain footprint are used to get its elevation and variation. Explanations are now added' The interpolation is performed with linear interpolation in time and nearest neighbor in space. … For each OCO-2 footprint, all SRTM grid points within the boundary are collected to get mean surface elevation and its variation. '.

C24- p4 l23: Your initial guess for CO2 and CH4 comes from different years, therefore it is subject to inter-annual variability. What is the sensitivity of your retrieval to this first guess?

R24-The annual variability of prior CO2 column is not considered but the effect of the prior is very small so we are convinced this is not a problem.

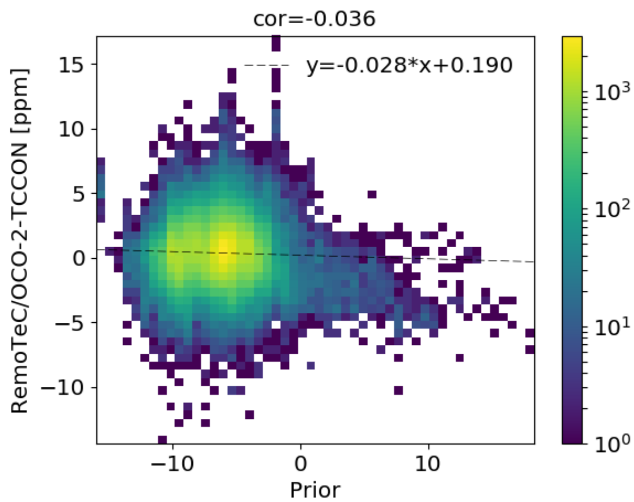

Figure 2. Dependency between XCO_2 difference and prior variation (unit ppm).

ref1: Butz, A., Guerlet, S., Hasekamp, O., Schepers, D., Galli, A., Aben, I., Frankenberg, C., Hartmann, J., Tran, H., Kuze, A., Keppel-Aleks, G., Toon, G., Wunch, D., Wennberg, P., Deutscher, N., Griffith, D., Macatangay, R., Messerschmidt, J., Notholt, J. and Warneke, T. (2011). Toward accurate CO2 and CH4 observations from GOSAT. Geophysical Research Letters, 38 (14), 1-6.

#reviewer2

This paper is describes the relatively straightforward application of the RemoTeC retrieval algorithm to data from the Orbiting Carbon Observatory-2 (OCO-2). RemoTeC was written to retrieve CO 2 and CH 4 column-average concentrations from the Greenhouse Gases Observing Satellite (GOSAT), and has been improved and validated over the years, as described in a number of publications. The authors have applied this mature algorithm to OCO-2 data to retrieve CO 2 (OCO-2 does not have the CH 4 band that GOSAT possesses), and find that after a few slight modifications, the error statistics of OCO-2 retrievals vs. ground truth data compare favorably both to the operational OCO-2 product as well as to RemoTeC retrievals of CO2 from GOSAT.

C-General Comments

The paper is useful in that it shows that the RemoTeC algorithm can be successfully applied to OCO-2, though it is relatively dry and offers few new physical insights into sources of error/bias in the OCO-2 measurements. However, is it worthwhile piece of work, and I recommend publication after making some minor revisions. My only main comment on the paper has to do with the filtering and bias correction, for which the bottom-line recipes are given. Some more information would be welcome. For instance, what other parameters were investigated for bias correction or filtering, such as the 1/(size parameter) variable used in GOSAT bias correction (Guerlet et al, 2013b)? Was the ω s parameter of Guerlet et al. (2013b) found not to be useful for OCO-2, even though it was for GOSAT? A figure similar to that of Figure 11 in Guerlet et al. (2013b) would be very useful here to see how similar/different GOSAT vs. OCO-2 retrieval biases are. Also, how stringent were your filters overall –did you filter out 10% L2-processed soundings, 50%, etc? How was this different over land and ocean? A throughput map would be useful.

R-The correlations of XCO2 difference with other parameters as used for GOSAT are now shown in Figure S1 in attachment. We tried the potential bias correction parameter (aerosol size, reff) as previously used by GOSAT retrievals. However, as can be seen in the bottom right panel of **Fig.S1** in 'Supporting Information' (SI) there is no clear dependency between this parameter.

For the overall throughput, we add in the paper "The overall L2-processed throughput is around 15%. When estimated separately, the percentages are 15.8%, 14.0% and 16.0% for target, land and ocean soundings, respectively."

C1- P2, L24: “XCO2 retrievals with this level of accuracy [<1%] can provide valuable information on...sources and sinks...” No! 1% = 4 ppm. We know that regional biases even 1 ppm (0.25%) in XCO2 are too large (Chevallier et al, 2014). Please modify or remove this statement.

R1-Modified. The statement now becomes " The XCO2 derived from GOSAT has an accuracy in the order of a few tents of a percent. XCO2 retrievals with this level of accuracy can provide valuable information on the variation of CO2 ."

C2-P3, L2: “by aerosols and cirrus.” Do water clouds not have any effect on scattering? I suggest changing this statement to “by aerosols and clouds.”

R2-modified.

C3-P3, 1 st paragraph. The authors describe a number of XCO2 retrieval algorithms but this list is certainly not exhaustive. There are the BESD and FOCAL retrievals from M. Reuter, the TanSAT retrieval from D. Yang, and various versions of the PPDF retrieval of Oshchepkov and Bril. You should either cite these or make clear that you are not exhaustively listing all available retrievals.

R3- Indeed, we are not trying to list all available retrieval algorithms so we use the word 'including'.

C4- P4, L22: "barometric law". Do you not mean the hypsometric equation (which combines the ideal gas law with the hydrostatic equation). They may be equivalent, I'm not entirely sure. But usually in this context, it is referred to as the hypsometric equation.
R4- Modified.

P4, L23: Are your priors adjusted for the secular growth rate of CO2 (since you just say you use CT from 2013)? Seems like you should, or you could probably introduce an artificial trend in your retrievals.
R5- No, for now, the growth rate is not considered in the prior. It is important to note that the retrieval results are hardly affected by the prior, see Figure 2.

P5, L20: Does Sy include any estimate of forward model error, as you previously implied it might (P5, L2). Similar are the noise estimates taken from the OCO-2 suggested formulation, or do you calculate your own noise estimates somehow?
R6-Sy only include noise estimates from the OCO-2 suggested formulation. Modified to be clear.

P6, L9-10: Please discuss whether the per-band radiance offsets were needed for GOSAT. My understanding is that they were needed for band 1, but not the other two bands. You could instead bring this up in section 4.3 as well, but I think it's important to contrast this need for the offsets in OCO-2 vs. that of GOSAT. For instance – I was thinking that maybe you needed them because your retrieval doesn't explicitly retrieve cirrus, so it would be difficult to retrieval soundings with a cirrus layer overlying a thin aerosol layer, which is a pretty common situation. Retrieval the 3 per-band offsets would be a pretty easy way to fake it. But that would likely then also be needed for GOSAT. Some discussion on this would be useful.
R7- For GOSAT the intensity offset fitting is only needed for the O2A band but not for the SWIR bands. This suggests that the offset corrects for an instrumental artefact rather than a retrieval artefact. The state vector differences between OCO-2 and GOSAT are now added in 4.3 section.

P7, L14: χ2 is the symbol usually referred to as the total chi-squared. What you show is much more similar to the "reduced chi-squared", which is the total chi- squared divided by the number of degrees of freedom (# channels - # retrieved parameters). You really are giving the mean chi-squared per channel. You should make this clear, and that a value around unity would indicate a fit that is in line with the noise. Values consistently higher than unity mean there are the systematic errors in the forward model that are not able to be fitted away.
R8- Indeed, χ2 is the "reduced chi-squared ". Modified accordingly in the paper.

P8, top: In the discussion of using the SWIR-1 chi-squared as a bias correction parameter, it would be nice to lengthen this discussion. Does SWIR-2 chi-squared perform similarly? Other parameters? Mention that r=0.2 means that 0.04 percent of the variance is explained (or it will reduce the standard deviation by about 2%). Why do you include the offset "d" parameter when you already include a global bias correction? They would be directly related to each other. Does this multiplicative formula (equation 4) work better than an additive equation? Finally, it would be valuable if you could speculate on why this parameter seems to be correlated with the bias over land. And perhaps on why it is NOT correlated with the bias over water. Are the chi-squared values much lower over water? Finally, what is the spatial distribution of this parameter? Is it highly scattered or does it seem to remove coherent regional biases?

R9- For bias correction, using SWIR-2 chi-squared gives similar results as using SWIR-1 chi-squared when we look at some overall statistics like station-to-station bias, or standard deviation. Using other parameters like those listed in Figure S1, the performance is different and can increase the station-to-station bias. Indeed, the goal of "d" in the bias correction is to correct a global bias. We tried to keep the bias correction purely multiplicative, since the leading scaling term would just link the spectroscopic calibration to the in-situ calibration. The performance is more or less the same with an additive equation.

The reason why the SWIR-1 chi-squared is highly correlated with the bias over land but not with that over ocean is probably related to the fact that high chi2 values over land are often related to bright surfaces. We know that retrieving aerosol over bright land surface is challenging. What we also see here is that SWIR-1 chi-squared is highly correlated (cor is around 0.75) with land surface albedo. However, using albedo directly to do the bias correction can NOT achieve similar performance and will make some statistics worse, for example seasonal variations. So, apart from bright surfaces, the bias correction with chi2 corrects XCO2 retrievals for cases where the forward model is less capable of fitting the measurements. By doing the correction, as we can see in the paper, we can reduce regional biases since the station-to-staion bias become less. For ocean glint, as we mentioned, aerosols play a less important role and mainly act as an extinction layer. Thus, we cannot see similar feature with land retrievals.

P9, L10: Some comments on why the effect of the bias correction is largest for those 3 stations would be welcome. It seems like it should be substantial for all over-land stations, unless the chi-squared values were just worse for those stations. My guess is that your chi-squared is going to be correlated with SNR or surface albedo, and brighter surfaces will have larger corrections. If you plotted the mean correction on a map, this would probably become obvious.
R10- Indeed, the chi-squared is highly correlated (correlation coefficient is around 0.75) with surface albedo. This could be partly attributed to aerosols since it is difficult to account scattering effects of aerosols over bright surfaces. We added a comment with the reason for the large correction effect for the 3 stations, " This happens due to that the goodness of fit is highly correlated with surface albedo and thus make the corrections apparently to regions with large albedos.".

Section 4.3 As mentioned before, contrast with the offset approach for GOSAT. Is the behavior of the fitted radiance offsets similar over land and ocean? How correlated are the fitted offsets for the 3 bands? (either in absolute terms, or relative to the mean radiance in their respective bands) If they are highly correlated, or not, that would give you a clue what they are correcting for (either cirrus, as I hypothesized earlier, or some instrument effect that is particular to OCO-2, and perhaps not GOSAT).
R11- The fitted radiance offsets are similar in retrievals over land and ocean. The intensity offsets for the 3 bands are moderately correlated with each other (around 0.35).

P11, top: Are the GOSAT vs. OCO-2 error statistics vs. TCCON similar for both land and ocean soundings?
R12- It is difficult to compare OCO-2 ocean retrievals to that of GOSAT because the collocated TCCON sites are quite limited (4 stations).

Figures: in many of the figures, the font sizes make reading some of the text difficult (axis labels, bias numbers , TCCON site names, etc). Please try to make them bigger to increase legibility.

R13-Thanks for the suggestion. We updated this in the revised manuscript.

Technical comments

P4, various: spectral samplings à spectral samples

P5, L10: “radiative transfer model Hasekamp...” à “radiative transfer model (Hasekamp...”

P10, L8: proportional mis-spelled

R14- modified.

Carbon dioxide retrieval from OCO-2 satellite observations using the RemoTeC algorithm and validation with TCCON measurements

Lianghai Wu[1], Otto Hasekamp[1], Haili Hu[1], Jochen Landgraf[1], Andre Butz[2,3], Joost aan de Brugh[1], Ilse Aben[1], Dave F. Pollard[4], David W. T. Griffith[5], Dietrich G. Feist[6], Dmitry Koshelev[7], Frank Hase[8], Geoffrey C. Toon[9], Hirofumi Ohyama[10], Isamu Morino[10], Justus Notholt [11], Kei Shiomi[12], Laura Iraci[13], Matthias Schneider[15], Martine de Maziére [14], Ralf Sussmann[15], Rigel Kivi[16], Thorsten Warneke[11], Tae-Young GOO[17], and Yao Té[7]

[1]SRON Netherlands Institute for Space Research, Utrecht, The Netherlands
[2]Institute of Atmospheric Physics, Deutsches Zentrum für Luft- und Raumfahrt e.V. (DLR), Wessling-Oberpfaffenhofen, Germany
[3]Meteorologisches Institut, Ludwig-Maximilians-Universität (LMU), Munich, Germany
[4]National Institute of Water and Atmospheric Research Ltd (NIWA), Lauder, New Zealand
[5]University of Wollongong, Wollongong, Australia
[6]Max Planck Institute for Biogeochemistry, Jena, Germany
[7]LERMA-IPSL, Sorbonne Universités, UPMC Univ Paris 06, CNRS, Observatoire de Paris, PSL Research University, 75005, Paris, France
[8]Karlsruhe Institute of Technology (KIT), IMK-ASF, Karlsruhe, Germany
[9]Jet Propulsion Laboratory, California Institute of Technology, Pasadena, California, USA
[10]National Institute for Environmental Studies (NIES), Tsukuba, Japan
[11]University of Bremen, Bremen, Germany
[12]Japan Aerospace Exploration Agency, Tsukuba, Japan
[13]NASA Ames Research Center, Moffett Field, CA, USA
[14]Royal Belgian Institute for Space Aeronomy, Brussels, Belgium
[15]Karlsruhe Institute of Technology (KIT), Institute of Meteorology and Climate Research (IMK-IFU), Garmisch Partenkirchen, Germany
[16]Finnish Meteorological Institute, Sodankylä, Finland
[17]National Institute of Meteorological Research, Seoul, Republic of Korea

Correspondence to: Lianghai Wu (l.wu@sron.nl)

Abstract.

In this study we present the retrieval of the column averaged dry air mole fraction of carbon dioxide (X_{CO_2}) from the Orbiting Carbon Observatory-2 (OCO-2) satellite observations using the RemoTeC algorithm, previously successfully applied to retrieval of greenhouse gas concentration from the Greenhouse Gases Observing Satellite (GOSAT). The X_{CO_2} product has been validated with collocated ground based measurements from the Total Carbon Column Observing Network (TCCON) for almost 2 years of OCO-2 data from September 2014 to July 2016. We found that fitting an additive radiometric offset in all three spectral bands of OCO-2 significantly improved the retrieval. Based on a small correlation of the X_{CO_2} error over land with ~~fit residuals~~goodness of fit, we applied an a posteriori bias correction to our OCO-2 retrievals. In ~~daily~~ overpass averaged results, X_{CO_2} retrievals have a standard deviation ~ 1.30 ppm and a station-to-station variability of ~ 0.40 ppm among collocated

TCCON sites. The seasonal relative accuracy (SRA) has a value of 0.52 ppm. The validation shows relatively larger difference with TCCON over high latitude areas and some specific regions like Japan.

1 Introduction

Carbon dioxide (CO_2) concentration is rapidly increasing in the atmosphere due to fossil fuel combustion and deforestation (Prentice et al., 2001). This can lead to significant changes in climate (Cox et al., 2000; Caldeira and Wickett, 2003). Any mitigation strategy to reduce CO_2 in the atmosphere requires a better understanding of the global carbon cycle, especially, identifying carbon dioxide emissions from both natural and anthropogenic sources and sinks that absorb carbon dioxide. Our ability to quantify sources and sinks of CO_2 is still insufficient due to the sparseness of current ground-based stations (Gurney et al., 2002; Patra et al., 2003; Houweling et al., 2004; Bösch et al., 2006; Baker et al., 2010).

To get a better understanding of the spatial and temporal pattern of sources and sinks of CO_2, efforts have been made to retrieve X_{CO_2} from satellite observations. The thermal infrared observations of CO_2 from instruments like the Atmospheric Infrared Sounder (AIRS), the Tropospheric Emission Spectrometer (TES) and the Infrared Atmospheric Sounding Interferometer (IASI) can provide CO_2 measurements at altitudes between 5 and 15 km (Chédin et al., 2002; Engelen et al., 2004; Crevoisier et al., 2009). These measurements have a limited sensitivity to CO_2 in the lower troposphere where CO_2 sources and sinks are located. Satellite observations measuring in the short-wave infrared (SWIR) spectral range, however, are sensitive to CO_2 down to the Earth's surface in the absence of clouds and so this spectral range is used to measure X_{CO_2} by several space missions. The SCanning Imaging Absorption spectroMeter for Atmospheric CHartographY (SCIAMACHY), operational between 2003 and 2012, is the pioneering instrument measuring X_{CO_2} from the SWIR spectra with sensitivity in the boundary layer (Buchwitz et al., 2005). Reuter et al. (2011) showed that accurate X_{CO_2} can be inferred from SCIAMACHY observations, taking atmospheric scattering processes into account in the retrieval. The Greenhouse Gases Observing Satellite (GOSAT), in orbit since January 2009, is the first satellite primarily dedicated to monitor global atmospheric levels of CO_2 and CH_4 from space (Yokota et al., 2009). The X_{CO_2} derived from GOSAT has an accuracy ~~well below 1.0% (Butz et al., 2011; Guerlet et al., 2013b; Kulawik et al., 2017)~~in the order of a few tents of a percent (Butz et al., 2011; Guerlet et al., 2 X_{CO_2} retrievals with this level of accuracy can provide valuable information on the ~~behavior of sources and sinks~~ variation of CO_2 (Rayner and O'Brien, 2001; Houweling et al., 2004; Guerlet et al., 2013a; Basu et al., 2014; Detmers et al., 2015). In July 2014, NASA's Orbiting Carbon Observatory-2 (OCO-2) satellite was successfully launched. OCO-2 is designed with three standard observational modes (nadir, glint and target) for accurate monitoring of the geographic distribution of carbon dioxide sources and sinks on a regional scale (Crisp et al., 2004). By taking advantage of the target mode where many observations are acquired over ground-based validation sites, the biases in the X_{CO_2} retrievals from OCO-2 measurements can be accurately evaluated. Furthermore, with a spatial sampling size of about 3 km^2, the number of cloud-free X_{CO_2} OCO-2 observations exceeds significantly those of previous missions.

One of the main challenges of X_{CO_2} retrieval from SWIR satellite measurements is to characterize the light path through the atmosphere affected by atmospheric scattering and surface reflection (Aben et al., 2007). For this purpose, current missions include measurements in the near infrared (NIR) spectral range covering the O_2 A absorption band. Measurements in the NIR and SWIR spectral bands allow for the simultaneous retrieval of carbon dioxide concentration with proper accounting of scattering properties introduced by aerosol or cirrusaerosols or clouds. Several algorithms have been developed to retrieve CO_2 from NIR/SWIR measurements from space, including the differential optical absorption spectroscopy (DOAS) retrieval method developed for the retrieval of SCIAMACHY (Buchwitz et al., 2000; Hönninger et al., 2004; Reuter et al., 2010), the algorithm developed at the National Institute for Environment Studies (NIES) for GOSAT observations (Yoshida et al., 2011), the Atmospheric CO_2 Observations from Space (ACOS) retrieval algorithm developed for the OCO instrument and later applied to the GOSAT and OCO-2 observations (O'Dell et al., 2012; Crisp et al., 2012), the algorithm developed in the University of Leicester (UoL) (Boesch et al., 2011; Jung et al., 2016), and the RemoTeC algorithm developed by SRON Netherlands Institute for Space Research and Deutsches Zentrum für Luft- und Raumfahrt e.V. (DLR) (Hasekamp and Butz, 2008; Butz et al., 2011; Guerlet et al., 2013b).

The operational X_{CO_2} data product of the OCO-2 mission is derived with the ACOS algorithm and validated against ground-based measurements (Wunch et al., 2017) and a dataset is avaliable available for assessing regional-scale sources and sinks (Eldering et al., 2017). To enhance the reliability and confidence of the data product, however, analyzing the data with independent algorithms is essential. For example, in the greenhouse gas project of ESA's Climate Change Initiative (GHG-CCI) extensive comparisons were made between different X_{CO_2} retrieval algorithms which showed similar results when comparing with TCCON data. However, in other regions the differences were sometimes significantly larger (Dils et al., 2014). In this paper, we adapt and apply the RemoTeC retrieval algorithm, previously applied to the GOSAT measurements, to OCO-2 measurements obtained under nadir, glint and target modes and evaluate the X_{CO_2} retrieval data quality with collocated ground based measurements from the Total Carbon Column Observing Network (TCCON) (Wunch et al., 2011a). To screen out too challenging soundings (i.e. clouds, high aerosol loadingsloading, large spectral uncertainties) we optimized the a posteriori data filtering and developed an X_{CO_2} bias correction based on spectral fitresiduals. goodness of fit. We expect that application of RemoTeC to OCO-2 data will lead to a better understanding to the capabilities and limitations of the OCO-2 instrument and the operational level-2 data product. Furthermore, we see this work as a first step towards processing a larger data set with RemoTeC.

The paper is organized as follows: Section 2 describes the OCO-2 data and Section 3 introduces the RemoTeC full physics retrieval algorithm including cloud screening and adjustments specific to OCO-2 type of measurements. In Section 4, we evaluate our retrieval results using collocated TCCON measurements. Here, the effect of bias correction is also discussed. To further evaluate the RemoTeC/OCO-2 retrievals, section 5 discusses the TCCON validation of X_{CO_2} data product from ACOS/OCO-2 and RemoTeC/GOSAT retrievals. Finally, Section 6 concludes the paper.

2 Data

The OCO-2 satellite provides measurements of sunlight backscattered by the Earth's surface and atmosphere in three channels including the molecular oxygen (O_2) A-band (around 0.765 μm, NIR), a weak CO_2 band (around 1.61 μm, SWIR-1) and a strong CO_2 band (around 2.06 μm, SWIR-2) with a spectral resolution of ~ 0.042, ~ 0.076 and ~ 0.097 nm for the three bands, respectively, defined as the full-width at half maximum (FWHM) of the instrument spectral response. Each FWHM is oversampled over-sampled by a factor 2 to 3 in the direction of dispersion. In each band, a linear polarizer is mounted in front of the imaging spectrometer and selects polarization vector parallel to the entrance slit. During operation, OCO-2 can collect observations with high signal-to-noise ratios under nadir, glint and target modes and each sounding provides measurements in 8 footprints adjacent to each other. The typical size of one footprint is around 1.3 km $\times$ 2.25 km under the nadir observation mode and can be a bit larger (around 3 km^2) for the other modes (Crisp et al., 2017).

In this study, we use version 7 OCO-2 data for the period September, 2014 to July, 2016. These data include observations obtained under nadir, glint and target observation modes. A few percent of the pixels of the OCO-2 detectors show performance anomalies (Crisp et al., 2017) and so we exclude the corresponding spectral samplings samples using the mask information provided in the L1b files. Finally, only spectra are processed where at least half of the spectral samplings samples passes this quality check.

For validation purpose, we focus on satellite observations that are collocated with measurements from TCCON, which is a global network of ground-based instruments that can measure X_{CO_2} in the atmosphere (Wunch et al., 2011a). The X_{CO_2} measured by TCCON has an uncertainty better than 0.25% (~ 1 ppm) (Wunch et al., 2015). More information on TCCON sites including locations and operational status can be found at https://tccon-wiki.caltech.edu/. The collocation criteria between OCO-2 measurements and TCCON measurements include a geographical distance less than 5 degrees in both latitude and longitude and a time difference less than 2 hours. Due to the high spatial sampling of OCO-2 (24 spectra per second over the swath), there are generally more than 150 cloud-screened spectra available for each collocated TCCON measurement. In this case, we use a maximum of 150 nadir or glint spectra, which are spatially closest to TCCON site, while for target observations we select those obtained with a viewing zenith angle smaller than 30°. This viewing zenith angle restriction has only been applied for target observations for time efficiency.

In addition to the OCO-2 spectra, the retrieval algorithm requires information on vertical profiles of pressure, temperature, humidity and surface wind speed, which are interpolated from the ECMWF (European Centre for Medium-Range Weather Forecasts) high resolution 10-day forecast analysis data on a $0.125° \times 0.125°$ latitude $\times$ longitude grid. The interpolation is performed with linear interpolation in time and nearest neighbour in space. The surface elevation information of the OCO-2 footprint is extracted from the 90 m digital elevation data of NASA's Shuttle Radar Topography Mission (SRTM) (Farr et al., 2007). For each OCO-2 footprint, all SRTM grid points within the boundary are collected to get mean surface elevation and its variation. We extrapolate the lowest ECMWF pressure point to the surface elevation provided by the SRTM data using the barometric lawhypsometric equation. To provide the algorithm initial guess of the CO_2 vertical concentration profiles and the CH_4 total column at each location, we use data from CarbonTracker and TM5 model for the year 2013 and 2010 (Peters et al., 2007; Houweling et al., 2014), respectively. The high-resolution solar irradiance data by Dr. R. Kurucz (http://kurucz.harvard.edu/sun/irradiance2008/) is used as reference solar spectrum in the forward radiative transfer model.

3 Method

The RemoTeC algorithm has been described in detail by Hasekamp and Butz (2008); Butz et al. (2009, 2010) and has been applied for CO_2 and CH_4 retrievals from GOSAT measurements (Butz et al., 2011; Schepers et al., 2012; Guerlet et al., 2013b). For OCO-2 application, the two most important algorithmic modifications are: (1) a vector radiative transfer model (LINTRAN V2) is employed in the retrieval scheme (Hasekamp and Landgraf, 2002, 2005a; Schepers et al., 2014); (2) Aerosol scattering effects are taken into account for ocean glint retrievals.

In the following, we assume that the OCO-2 radiance measurements $\boldsymbol{y}$, comprising of measurements in all three bands, can be described by a forward radiative transfer model $\boldsymbol{F}$ via,

$$\boldsymbol{y} = \boldsymbol{F}(\boldsymbol{x}, \boldsymbol{b}) + \boldsymbol{e} \tag{1}$$

Here, $\boldsymbol{x}$ is the state vector containing all parameters to be retrieved and $\boldsymbol{b}$ includes a set of auxiliary input parameters. The error term $\boldsymbol{e}$ contains uncertainties in both instrument and forward model. To infer X_{CO_2}, RemoTeC resolves Eq.1 with respect to the state vector $\boldsymbol{x}$.

The OCO-2 instrument measures the backscattered sunlight in a single polarization direction, and so the forward model for spectral sampling i reads,

$$F_i(\boldsymbol{x}, \boldsymbol{b}) = m_{11} I_i + m_{12} Q_i + m_{13} U_i \tag{2}$$

where I_i, Q_i and U_i are the first three stokes parameters of a line-by-line top of the model atmosphere spectrum convolved with the OCO-2 instrument spectral response function. The elements of the Muller matrix m_{11}, m_{12}, and m_{13} describe the instrument polarization sensitivity depending on the illumination and observing geometries of the OCO-2 instrument. For the simulation of the line-by-line spectra, we employ the LINTRAN vector radiative transfer model ~~Hasekamp and Landgraf (2002, 2005a); Schepers~~
To simulate efficiently the spectral dependence of the Stokes parameter I, Q and U, defined at the top of the model atmosphere, the multiple scattering calculations are performed following the k-binning approach of Hasekamp and Butz (2008) while the single scattering is calculated line-by-line. In the algorithm, the model atmosphere is divided into 36 sub-layers for the radiative transfer calculation and further divided into 72 sub-layers for absorption cross-section calculation which is highly dependent on temperature and pressure.

Since the measurement $\boldsymbol{y}$ does not contain sufficient information to retrieve all elements of state vector $\boldsymbol{x}$, the algorithm employs a Phillips-Tikhonov regularization scheme to solve the minimization problem iteratively (Phillips, 1962; Tikhonov, 1963; Hasekamp and Landgraf, 2005b),

$$\hat{\boldsymbol{x}} = \min_{\boldsymbol{x}} (\|\boldsymbol{S}_y^{-\frac{1}{2}} (\boldsymbol{F}(\boldsymbol{x}) - \boldsymbol{y})\|^2 + \gamma \|\boldsymbol{W}(\boldsymbol{x} - \boldsymbol{x}_a)\|^2), \tag{3}$$

where $\boldsymbol{S}_y$ is the diagonal measurement error covariance matrix that contains the measurement error ~~estimate~~estimates of OCO-2, $\boldsymbol{x}_a$ is a prior state vector, γ is the regularization parameter and $\boldsymbol{W}$ is the weighting matrix making the side constraint dimensionless. The value for γ is fixed such that the degree of freedom for signal (DFS) for the carbon dioxide profile is in the range 1.0-1.5. To avoid diverging retrievals, following a Gauss-Newton scheme (Rodgers, 2000) a filter factor ($\Lambda = \frac{1}{1+\xi}, \xi \geq 0$) is also introduced to limit the update of the state vector per iteration step. More details on this aspect of the RemoTeC implementation can be found in Butz et al. (2012). The retrieval is considered successful when following conditions are all met: (1) the update of the state vector $\boldsymbol{x}$ become smaller than its theoretical uncertainty; (2) the step-size parameter ξ has reached 0; (3) the state vector elements have never reached unrealistic values during the iteration.

The forward model assumes the land surface reflection to be Lambertain, whereas ocean surface reflection is modeled using a wind speed dependent Cox-and-Munk reflection model (Cox and Munk, 1954) with a wavelength dependent Lambertian term added to it. Oxygen absorption lines in the A band are calculated by a spectroscopic model that accounts for line mixing and collision-induced absorption processes (Tran and Hartmann, 2008). Absorption lines of CO_2 are ~~modelled~~ modeled accordingly to the HITRAN 2008 spectroscopic data base, by taking line-mixing into account (Rothman et al., 2009; Lamouroux et al., 2010). HITRAN 2008 is also used to model absorption lines of CH_4 and H_2O assuming a Voigt lineshape model. In the retrieval, we treat aerosol as spherical particles with a constant refractive index $(1.400 - 0.003i)$ over the whole OCO-2 spectral range. The aerosol size distribution is described by a power law function $(n(r) \propto r^{-\alpha_s})$ with size parameter α_s while the aerosol height profile is assumed to be Gaussian with a central height parameter z_s and a fixed geometric width of 2 km. Based on this aerosol model, we calculate the optical properties of aerosol particles using the tabulated kernels of Dubovik et al. (2006).

In the retrieval, the state vector $\boldsymbol{x}$ includes the 12-layer profile of CO_2 sub-column number densities along with total column number densities of interfering absorbers CH_4 and H_2O, surface parameters including a second order spectral dependence of the Lambertian surface albedo in all OCO-2 bands. Moreover, $\boldsymbol{x}$ contains the aerosol size parameter α_s of the power-law distribution, the total column density of aerosol particles, and the central height parameter z_s of the Gaussian height distribution. Finally, in all three bands we infer an intensity offset, a first order spectral shift of the Earth radiance spectrum and a spectral shift of the solar reference spectrum. To initialize the retrieval, we choose an aerosol total column, which corresponds to an aerosol optical depths of 0.1 in the NIR spectral band, a size parameter $\alpha_s = 4.5$ and an aerosol layer height $z_s = 3000$ m. Table 1 lists the state vector elements and prior values, if applicable, considered in the retrieval. After convergence, the spectral fit residuals are generally less than 1.0% with a typical reduced chi squared of 3.0.

Since clouds are not considered in RemoTeC, a cloud screening of the OCO-2 data is required before performing full physical retrieval. For this purpose, we ~~apply the screening approach similar to Taylor et al. (2016) in our algorithm~~ implemented a fast non-scattering retrieval as part of the RemoTeC and compare columns of O_2, CO_2 and H_2O, which are retrieved independently ~~for a non-scattering atmosphere~~ from the NIR, SWIR-1, and SWIR-2 bands of OCO-2, respectively. When neglecting cloud and aerosol scattering a large deviation can be introduced between CO_2 and H_2O columns retrieved from SWIR-1 and SWIR-2 bands due to different light path sensitivity. Similarly, for scenes with larger photon path-length modification, the retrieved O_2 column will deviate more from the O_2 column provided by the ECMWF. Cloud filtering are performed by applying the following criteria: $0.885 < O_2^{ret}/O_2^{ecmwf} < 1.020$, $0.990 < CO_2^{swir1}/CO_2^{swir2} < 1.035$ and $0.950 < H_2O^{swir1}/H_2O^{swir2} < 1.060$. Here, around 30% of total soundings are identified as cloud-free cases by the cloud screening. If estimated separately, the percentage of clear soundings are 24%, 28% and 34% for target, land and ocean glint observations, respectively. For now, we mainly use those ratios as a option to filter cloud contaminated cases for the full physical retrieval. Apart from cloud screening, observations with solar zenith angle $> 70°$ and large surface roughness (standard deviation of surface elevation > 75 m) are also excluded before performing the operational retrievals.

4 Validation with TCCON

In this section, we evaluate the X_{CO_2} retrieved from OCO-2 measurements using the RemoTeC algorithm against ground-based measurements at a comprehensive set of TCCON stations. Figure 1 shows an example of validation between RemoTeC/OCO-2 retrievals and TCCON measurements over Lamont and Darwin stations. ~~To~~ Here, we can see that RemoTeC/OCO-2 retrievals can well capture the seasonal X_{CO_2} variation features of both northern hemisphere and southern hemisphere. To better evaluate our retrieval quality, we use the bias (b) as the mean difference between collocated TCCON and OCO-2 retrievals, the sounding precision (σ) as the standard deviation of the difference and the station-to-station variability (σ_s) as the standard deviation of the biases for different TCCON stations. Here, retrievals over land and ocean are evaluated separately. The separation is due to the fact that land and ocean surface reflections are modeled differently. Land retrievals include observations obtained under nadir and glint modes and ocean retrievals only include observations under glint mode. Target mode observations, mostly performed coincidentally around TCCON sites over land, are evaluated separately. Moreover, the standard deviation over all seasonal bias results, known as "seasonal relative accuracy"(SRA) introduced by Dils et al. (2014), are also derived for all three types of retrievals. The SRA value is a good indicator of the variability of the bias in both space and time. In the following validation, we assume that TCCON measurements themselves are consistent over all stations with a station-to-station variability of zero. However, as discussed by Kulawik et al. (2016); Buchwitz et al. (2017b), individual stations have a year-to-year variability of ~ 0.3 ppm and the overall TCCON X_{CO_2} uncertainty is around 0.4 ppm (1-sigma). Although some limitations may exist, TCCON measurements are the most appropriate validation data product for satellite observations. Here, we exclude stations located either close to source region such as Caltech or on very high latitude such as Eureka. Land retrievals obtained over Reunion Island, located within areas with significant topography and an active volcano, will also not be used for validation.

4.1 Filters and bias correction

We first compare our retrieval results with collocated TCCON data to establish a set of values for the filters shown in Table 2 to screen out retrievals with larger uncertainties. In our retrieval, around 83%, 81% and 72% of cloud-free cases successfully converge and, after applying the filters in Table 2, 66%, 50% and 47% of retrievals remain with good quality in cloud-screened target, land and ocean types of measurements, respectively. The overall L2-processed throughput is around 15%. When estimated separately, the percentages are 15.8%, 14.0% and 16.0% for target, land and ocean soundings, respectively.

Similar to the work of Butz et al. (2011); Guerlet et al. (2013b), we apply filters to reject retrievals with bad quality of fit ($\chi^2 > 7.0$, $\chi^2_{1st} > 7.0$ or not converged with number of iterations > 30), or with high aerosol loading ($\tau_{0.765} > 0.35$), or with extreme aerosol parameters ($\alpha_s < 3.5$, $\alpha_s > 8.0$ or aerosol ratio parameter > 300 m), or with surface types like snow or ice (blended albedo > 0.9). Here, the reduced χ^2 is defined as $1/N \sum_{i=1}^{N} (\frac{(y(i)-F(i)}{\delta_i})^2$, in which N is the number of measurements minus the degree of freedom for signal (DFS), $y(i)$ is the OCO-2 measurement, $F(i)$ is the simulated result and

δ_i is the uncertainty of the OCO-2 measurements. In OCO-2 retrievals, intensity offset parameters are fitted for all the three spectral windows and we use the ratio between retrieved intensity offset and mean spectral radiance to filter out soundings with larger spectral uncertainties. Here, target retrievals have the same filter settings as land retrievals.

Ocean glint measurements require different filter settings because of their different sensitivity due to unique viewing geometry and different surface properties. Moreover, in the measured radiance of ocean glint measurements, the contribution from aerosol scattering is negligible when compared with that from ocean surface reflection. As a consequence, the measured radiances are mainly sensitive to ocean reflection and aerosol layer extinction properties. Aerosol filter settings used here are different from land retrievals due to the limitation of aerosol information and aerosol parameters like particle size and layer height usually retain their prior values.

When comparing ~~our~~ individual retrieval results with collocated TCCON measurements, we look for possible ~~correlations~~ corrections of errors with instrumental, geophysical, meteorological and retrieved parameters. This correction should be valid for each single sounding and thus evaluated with individual results. In this paper, a positive bias means X_{CO_2} is overestimated by the RemoTeC/OCO-2 retrievals. Figure 2 shows that only a small overall bias of 0.31, 0.37, and 0.70 ppm exist in the RemoTeC/OCO-2 retrievals for target, land and ocean types of retrievals, respectively. Here, the dependency of difference between OCO-2 and TCCON with collocation distance and surface pressure is negligible. However, if we look at retrievals from 8 individual footprints within a swath separately, the X_{CO_2} retrievals show statistically significant differences on overall biases ranging from -0.25 to 0.65 ppm with a standard deviation of 0.3 ppm. These biases arise from uncertainties in the L1 processing depending on the viewing direction in across flight direction and have to be removed before performing an overall bias correction. To identify the footprint dependent biases, we use target mode observations when all 8 footprints in one sounding frame converged, which provides around 7000 available retrievals per footprint. By using a large amount of target observations we can reduce the uncertainties in the footprint-to-footprint bias estimation. Here, we assume a constant X_{CO_2} field in across track direction. The estimated swath-dependent biases, as shown in Fig 3, are directly subtracted from each footprint.

After removing the swath-dependent biases, a bias dependence on the ~~fit residual~~ χ^2 in SWIR-1 band is found for RemoTeC/OCO-2 retrievals over land. As shown in Fig. 4, a typical χ^2 in SWIR-1 band is around 2.0 and the correlation ~~cofficient~~ coefficient is 0.20. ~~This bias~~ Here, χ^2 in SWIR-1 and SWIR-2 bands are highly correlated with corresponding retrieved surface albedos. A possible explanation for the correlation between bias and χ^2 is that χ^2 correlates with surface brightness. For bright surfaces, the noise becomes small and some "constant" fit residuals show up. This "constant" fit residuals can be attributed to many factors like spectroscopic errors, inconsistent aerosol assumptions and instrument or algorithm uncertainties. ~~We~~ Here, we correct this bias by

$$XCO_2^{corr} = XCO_2(d + k \cdot {\chi^2}_{swir1}), \tag{4}$$

where the coefficients $k = -0.001261$ and $d = 1.001938$ are derived with a linear regression fit through the difference between individual retrievals and TCCON measurements. This correction reduces the error correlation with most parameters in Table 2 such as overall χ^2, surface albedo in the NIR band(albedo_NIR), solar zenith angle and degrees of freedom for signal, even though these parameters are not used in the bias correction and the remaining correlations with related parameters are generally less or around 0.100.15. After applying this bias correction the swath-dependent biases remains low around -0.1 ppm with a standard deviation of 0.01 ppm. Similar improvement can be achieved by using χ^2 in SWIR-2 band in the bias correction.

For ocean glint retrievals, we only subtract the swath-dependent bias and a constant bias of 0.65 ppm from the X_{CO_2} results. The constant bias is obtained by validating retrieval results with collocated TCCON measurements from sites as listed in Fig. 7. The X_{CO_2} swath-dependent bias for ocean glint observations is very similar to the one of X_{CO_2} target observations and so the same correction is applied.

Overall, with the bias correction in Eq. 4 the sounding precisions σ are slightly improved by ~ 0.1 ppm for land retrievals in Fig. 2. The land and ocean bias corrections are developed for reducing globally-relevant biases and thus geographically related or time dependent biases may remain in the results and need further investigation.

4.2 TCCON validation

For a detailed validation of the bias corrected X_{CO_2} product, we will evaluate the X_{CO_2} retrieved from OCO-2 target, land and ocean measurements using the RemoTeC algorithm for different TCCON stations separately. The average of the retrieved X_{CO_2} is compared with the corresponding TCCON average values. We exclude cases where less than 5 individual data points are available within 2 hours in either OCO-2 retrievals or TCCON data. To evaluate the retrieval quality, we take into account the bias (b_a), standard deviation (σ_a), station-to-station variability (σ_s) and seasonal relative accuracy (SRA) against TCCON measurements station by station. Here, the station-to-station variability is an important evaluation parameter known as a measure of regional-scale accuracy, which is most important for estimating CO_2 surface-to-atmosphere fluxes on regional scales. The SRA value further indicates the potential bias variation in both space and time. Moreover, we study the effect of the bias correction by analysing the retrieval performance station-by-station.

Figures 5, 6 and 7 show the overall comparisons between RemoTeC/OCO-2 retrievals after bias correction and TCCON measurements for target, land and ocean retrievals, respectively. In the daily overpass averaged results, the bias and standard deviation (b_a, σ_a) are (-0.07, 1.24), (0.00, 1.36), and (0.00, 1.20) ppm for target, land and ocean retrievals, respectively. Before bias correction, the mean biases are 0.51, 0.44 and 0.62 0.75 ppm for the above three type of retrievals, respectively. The bias correction mainly improves the mean bias though the standard deviations are also reduced by ~ 0.1 ppm for land retrievals.

Figure 8, 9 and 10 show the bias (b_a) at each TCCON site as a function of its latitude for the target, land and ocean types of retrievals. The mean ($\overline{b_a}$) and the standard deviation (σ_s) of all the biases are also derived. Stations with less than 5 valid points have been excluded from the analysis. The number of stations used in the validation are 10, 17 and 18 for target, land and ocean retrievals, respectively. Within those stations, most of them have a bias less than 0.5 ppm for both land and ocean retrievals.

In Fig. 8, the remaining X_{CO_2} bias for target observations varies from -0.81 ppm (Tsukuba, Japan) to 0.47 ppm (Lauder, New Zealand). The developed bias correction reduces the station-to-station variability from 0.54 ppm to 0.35 ppm. The effect of the bias correction is largest for Lamont, Dryden and Darwin stations (> 0.50 ppm on the mean station bias) while in other stations the difference is small. This happens due to that the goodness of fit are highly correlated with surface albedo and thus make the corrections apparently to regions with large albedos. Land retrievals as shown in Fig 9, validated among 17 stations, have a station-to-station variability of 0.41 ppm. The remaining bias varies from -0.66 ppm (Lamont, OK(USA)) to 1.03 ppm (Sodankyla, Finland). Here, most stations have similar biases as found for the corresponding target observations. The bias correction also helps to reduce the station-to-station variability for land retrievals although not that much. Among all the stations, Tsukuba station in Japan have relatively larger standard deviation of 2.07 ppm. For retrievals in Figs 8 and 9, there is a tendency that validations over stations in higher latitude areas have relatively larger biases in both northern and southern hemispheres. In addition, target observations have a smaller station-to-station variability than land observations although different TCCON stations are involved.

For ocean retrievals, since we only subtract swath dependent bias and a mean bias, the station-to-station variability (0.44 ppm) is the same before and after bias correction. The biases vary from -0.86 ppm (Saga, Japan) to 0.75 ppm (Bremen, Germany). There is no clear indication of latitude dependent bias variation.

Moreover, we investigated temporal variations in RemoTeC/OCO-2 X_{CO_2} retrievals. As showin in Fig.1, seasonal X_{CO_2} variation features in the northern hemisphere can be well captured by both RemoTeC/OCO-2 retrievals and TCCON measurements. At the southern hemisphere, the X_{CO_2} is more stable throughout the whole time range. Fig. 11 shows the time series of X_{CO_2} difference between TCCON measurements and X_{CO_2} retrievals from OCO-2 target, land and ocean types of measurements. At most stations, no time-dependent biases can be clearly observed. For some stations in the northern hemisphere like Sodankyla, Bremen and Paris, time-dependent features can also be attributed to inhomogeneous seasonal data distribution. There are some outliers in X_{CO_2} retrievals from both land and ocean glint observations, such as those at the Tsukuba over land and Lauder over ocean, that need further investigation.

Finally, we check the "seasonal relative accuracy"(SRA) which is derived for all three types of observations. For each station, all the data regardless of the year are sorted into four intervals of a calendar year. Table 3 summarizes seasonal bias per station, standard deviation of biases per season, seasonal variability ("Seas") and the SRA value. The derived SRA of 0.52 ppm is close to the requirement of 0.50 ppm as discussed by Dils et al. (2014). Here, the developed bias correction helps to improve the SRA from 0.60 to 0.52 ppm. In stations where seasonal variability can be caculated, the value is generally around 0.30 ppm except stations Rikubetsu (0.71 ppm) and Saga (0.43 ppm) in Japan. In Table 3 the SRA values are mainly driven by large negative biases from Rikubetsu, Tsukuba and Saga stations in Japan. Further investigations are needed to diagnose the remaining larger biases in certain season over stations in Japan.

4.3 Importance of intensity offset

As mentioned in section 3, the implementation of the RemoTeC algorithm, used in this study, fits an intensity offset for all three OCO-2 bands. In previous GOSAT retrievals we only fit intensity offset for the NIR band. To identify its importance, we performed the same retrieval as in Fig. 6 but without fitting intensity offset in the SWIR-1 and SWIR-2 bands. Figure 12 shows that without fitting intensity offsets in the SWIR-1 and SWIR-2 bands the validation exhibits a negative bias of -2.95 ppm and the standard deviation increased by ~ 0.5 ppm.

As shown in Fig 13, in the SWIR-1 and SWIR-2 bands the fitted intensity offsets are propotinal proportional to the mean radiance with a slope of 0.0025 and 0.0035, respectively. This slope is generally about two times larger than that of noise. Generally, the fitted intensity offset in these two bands are $\sim 0.4\%$ of the corresponding mean radiance. There are no clear time-dependent features in the fitted intensity offset. The intensity offset in the O_2 A band shows a less strong dependence on the signal level itself. Here, it could be a compensation to solar-induced chlorophyll fluorescence (SIF) since currently it is not fitted in the retrieval. Moreover, it could also be partly introduced by light reflection by degraded anti-reflection coating on the focal plane array (Crisp et al., 2017). However, this can not explain the amount of intensity offset retrieved in our algorithm for the SWIR-1 and SWIR-2 bands since for those channels much thicker and higher index anti-reflection coatings are used (Crisp et al., 2017). Potential causes could be straylight from reflection of nearby ground pixels or from components of the optical system.

5 Discussion

As we mentioned before, OCO-2 level-2 products delivered by the ACOS retrieval algorithm are also validated with collocated TCCON data by Wunch et al. (2017). Before comparing our results with the results in Wunch et al. (2017), we need to point out several differences of the validation approach by Wunch et al. (2017) and our study: (1) The considered time range of the study by Wunch et al. (2017) is from September, 2014 to January, 2017; (2) A collocation criterion of 5° in latitude and 10° in longitude is applied for most stations, but for Caltech and Dryden and those located on the southern hemisphere, a specific local collocation criterion is employed; (3) daily median values of both OCO-2 retrievals and TCCON are used for comparison; (4) observations over land under nadir and glint modes are validated separately;(5) the employed filter settings and bias corrections are also different from here.

Albeit For bias-corrected data, albeit with so many differences, we still see a lot of common aspects when looking at the standard deviation and station-to-station variability in Wunch et al. (2017). For example, for the results under warn level 11 (the best 50% of the total L2 data, see Mandrake et al. (2015) for more details on warn level) the standard deviation of the difference (OCO-2-TCCON) for land retrievals is around 1.3 ppm. Looking at station-to-station variability for ACOS land retrievals, the σ_s is ~ 0.45 ppm over 12 stations. For ocean glint retrievals, the σ_s is 0.46 ppm over 9 stations. These values are more or less the same, albeit a bit higher, as what we see in the validation in Figs. 9 and 10.

In order to perform a more direct comparison between ACOS and RemoTeC, we took the common data-points that passed quality filtering for both algorithms for the period under consideration of this study. In total, we collect 34560 individual retrievals collocated with 18 TCCON stations. These retrievals only take 31.0% of total land retrievals in Fig. 2 and which means we have quite different data coverage with ACOS/OCO-2. As expected, after bias correction, the results between ACOS and RemoTeC are similar with a bias, standard deviation, and station-to-station bias of -0.02 ppm, 1.36 ppm, 0.44 ppm in RemoTeC and 0.13 ppm, 1.31 ppm, 0.55 ppm in ACOS. However, when looking at the results before bias correction the differences are larger. Before bias correction, the overall bias and standard deviation are (0.58 ppm, 1.62 ppm) in RemoTeC/OCO-2 retrievals and (-1.38 ppm, 1.89 ppm) in ACOS/OCO-2 retrievals. When looking at overpass averaging results, in total

646 cases, RemoTeC/OCO-2 retrievals have a mean bias of 0.67 ppm with a standard deviation of 1.43 ppm meanwhile ACOS/OCO-2 retrievals have a mean bias of −1.04 ppm with a standard deviation of 1.53 ppm. The station-to-station biases are 0.47 ppm and 0.63 ppm for RemoTeC/OCO-2 and ACOS/OCO-2, respectively. The ACOS product depends much more on bias correction than RemoTeC. Possible reasons are the zero-level offset fits in RemoTeC that are not performed by ACOS or the difference in the treatment of aerosols.

X_{CO_2} retrievals from GOSAT measurements using the RemoTeC algorithm have also been validated with TCCON data (Butz et al., 2011; Guerlet et al., 2013b; Dils et al., 2014; Buchwitz et al., 2017b). There are several improvements on the RemoTeC/GOSAT X_{CO_2} retrieval quality since the first report by Butz et al. (2011). Here we will use the latest results over land reported by Buchwitz et al. (2017a). It should be noted that there are quite some differences between RemoTeC/GOSAT and RemoTeC/OCO-2 including instrument polarization sensitivity, collocation criteria, filtering options and so on. In the validation between RemoTeC/GOSAT X_{CO_2} retrievals and TCCON data, the sounding precision is 1.9 ppm with a station-to-station variability (estimated over 12 stations) of 0.43 ppm. The derived SRA is 0.51 ppm. Looking at those overall statistic values, there are no significant differences between X_{CO_2} retrievals from RemoTeC/OCO-2 and RemoTeC/GOSAT. Before bias correction, the major difference between RemoTeC/OCO-2 and RemoTeC/GOSAT is the overall bias (0.35 ppm .vs. −2.25). However, further investigation is needed to identify the difference between X_{CO_2} retrievals from those two satellites, especially over regions where TCCON data is not available.

6 Conclusions

In this paper, we extended and adapted the full physics retrieval algorithm RemoTeC, previously applied to GOSAT, for OCO-2 satellite measurements. The algorithm was applied to OCO-2 nadir, glint and target observations obtained over land and ocean (glint only). We defined both an a posteriori data filtering approach and bias correction as a function of the swath position by comparing with TCCON. Additionally, we introduced a linear bias correction for land observations as a function of the spectral fit quality. Comparison of the retrieved X_{CO_2} with collocated ground-based TCCON stations showed that for both land and ocean observations our retrieval results exhibit a residual bias less than 0.10 ppm with a standard deviation around 1.30 ppm (for ~~daily~~ overpass means) and a station-to-station variability variation around 0.40 ppm. Among the individual TCCON stations, the biases are generally less than 0.50 ppm. In land retrievals, middle to high latitude areas have relatively larger biases and in ocean retrievals no latitude-dependent bias can be clearly seen. The target observations have a station-to-station variability around 0.35 ppm which approaches the systematic error required for regional CO_2 source/sink determination (Chevallier et al., 2005; Houweling et al., 2010; Chevallier et al., 2014b, a). The better comparison with TCCON for target mode retrievals compared to regular land retrievals could be attributed to the fact that under the target mode the OCO-2 satellite is directly looking at the place where TCCON sites are located and this provides a better collocation and therefore prevents apparent biases caused by local X_{CO_2} variations. Time series validation indicates that RemoTeC/OCO-2 retrieval results can well capture the seasonal cycle of X_{CO_2} in both hemispheres and no time-dependent bias can be clearly observed in the retrieval. The seasonal relative accuracy investigated over 66 time intervals of collocated stations has a value of 0.52 ppm. Most of stations have a seasonal variability around 0.30 ppm except for those in Japan. For the X_{CO_2} retrieval from OCO-2 measurements, we see that intensity offsets need to be fitted for all three bands otherwise a larger bias (2.50 ppm) and standard deviation (0.50 ppm) would be introduced in the results.

7 Data availability

The OCO-2 data (version 7) used here were produced by the OCO-2 project at the Jet Propulsion Laboratory, California Institute of Technology, and obtained from the OCO-2 data archive maintained at the NASA Goddard Earth Science Data and Information Services Center (https://daac.gsfc.nasa.gov/). TCCON data were obtained from the TCCON Data Archive, hosted by the Carbon Dioxide Information Analysis Center (CDIAC) http://tccon.ornl.gov/ at that time. Since October 2017, the TCCON Data Archive is hosted by CaltechDATA, California Institute of Technology, CA (US), doi:10.14291/tccon.archive/1348407. The RemoTeC/OCO-2 X_{CO_2} retrievals used in this paper are available upon request from Lianghai Wu (l.wu@sron.nl).

Acknowledgements. This research was funded by the Netherlands Space Office as part of the User Support Programme Space Research under project ALW-GO/15-23. We are grateful to Université Pierre et Marie Curie, French space agency CNES and Région Île-de-France for their financial contributions as well as to Institut Pierre-Simon Laplace for support and facilities.

References

Aben, I., Hasekamp, O., and Hartmann, W.: Uncertainties in the space-based measurements of CO2 columns due to scattering in the Earth's atmosphere, Journal of Quantitative Spectroscopy and Radiative Transfer, 104, 450 – 459, https://doi.org/https://doi.org/10.1016/j.jqsrt.2006.09.013, http://www.sciencedirect.com/science/article/pii/S0022407306002342, 2007.

Baker, D. F., Bösch, H., Doney, S. C., O'Brien, D., and Schimel, D. S.: Carbon source/sink information provided by column CO_2 measurements from the Orbiting Carbon Observatory, Atmospheric Chemistry and Physics, 10, 4145–4165, https://doi.org/10.5194/acp-10-4145-2010, 2010.

Basu, S., Krol, M., Butz, A., Clerbaux, C., Sawa, Y., Machida, T., Matsueda, H., Frankenberg, C., Hasekamp, O. P., and Aben, I.: The seasonal variation of the CO2 flux over Tropical Asia estimated from GOSAT, CONTRAIL, and IASI, Geophysical Research Letters, 41, 1809–1815, https://doi.org/10.1002/2013GL059105, http://dx.doi.org/10.1002/2013GL059105, 2014.

Blumenstock, T., Hase, F., Schneider, M., Garcia, O. E., and Sepulveda, E.: TCCON data from Izana (ES), Release GGG2014.R0, TCCON Data Archive, hosted by CaltechDATA, https://doi.org/10.14291/tccon.ggg2014.izana01.R0/1149295, 2014.

Boesch, H., Baker, D., Connor, B., Crisp, D., and Miller, C.: Global characterization of CO2 column retrievals from shortwave-infrared satellite observations of the Orbiting Carbon Observatory-2 mission, Remote Sensing, 3, 270–304, 2011.

Bösch, H., Toon, G., Sen, B., Washenfelder, R., Wennberg, P., Buchwitz, M. d., De Beek, R., Burrows, J., Crisp, D., Christi, M., et al.: Space-based near-infrared CO2 measurements: Testing the Orbiting Carbon Observatory retrieval algorithm and validation concept using SCIAMACHY observations over Park Falls, Wisconsin, Journal of Geophysical Research: Atmospheres, 111, 2006.

Buchwitz, M., Rozanov, V. V., and Burrows, J. P.: A near-infrared optimized DOAS method for the fast global retrieval of atmospheric CH4, CO, CO2, H2O, and N2O total column amounts from SCIAMACHY Envisat-1 nadir radiances, Journal of Geophysical Research: Atmospheres, 105, 15 231–15 245, https://doi.org/10.1029/2000JD900191, 2000.

Buchwitz, M., de Beek, R., Burrows, J. P., Bovensmann, H., Warneke, T., Notholt, J., Meirink, J. F., Goede, A. P. H., Bergamaschi, P., Körner, S., Heimann, M., and Schulz, A.: Atmospheric methane and carbon dioxide from SCIAMACHY satellite data: initial comparison with chemistry and transport models, Atmospheric Chemistry and Physics, 5, 941–962, https://doi.org/10.5194/acp-5-941-2005, 2005.

Buchwitz, M., Dils, B., Boesch, H., Crevoisier, C., Detmers, D., Frankenberg, C., Hasekamp, O., Hewson, W., Laeng, A., Noël, S., et al.: ESA Climate Change Initiative (CCI) Product Validation and Intercomparison Report (PVIR) for the Essential Climate Variable (ECV) Greenhouse Gases (GHG) for data set Climate Research Data Package No. 4 (CRDP# 4), Version 5, 4, 253, 2017a.

Buchwitz, M., Reuter, M., Schneising, O., Hewson, W., Detmers, R., Boesch, H., Hasekamp, O., Aben, I., Bovensmann, H., Burrows, J., et al.: Global satellite observations of column-averaged carbon dioxide and methane: The GHG-CCI XCO 2 and XCH 4 CRDP3 data set, Remote Sensing of Environment, 2017b.

Butz, A., Hasekamp, O. P., Frankenberg, C., and Aben, I.: Retrievals of atmospheric CO 2 from simulated space-borne measurements of backscattered near-infrared sunlight: accounting for aerosol effects, Applied optics, 48, 3322–3336, 2009.

Butz, A., Hasekamp, O., Frankenberg, C., Vidot, J., and Aben, I.: CH4 retrievals from space-based solar backscatter measurements: Performance evaluation against simulated aerosol and cirrus loaded scenes, Journal of Geophysical Research: Atmospheres, 115, 2010.

Butz, A., Guerlet, S., Hasekamp, O., Schepers, D., Galli, A., Aben, I., Frankenberg, C., Hartmann, J.-M., Tran, H., Kuze, A., Keppel-Aleks, G., Toon, G., Wunch, D., Wennberg, P., Deutscher, N., Griffith, D., Macatangay, R., Messerschmidt, J., Notholt, J., and Warneke, T.: Toward accurate CO2 and CH4 observations from GOSAT, Geophysical Research Letters, 38, n/a–n/a, https://doi.org/10.1029/2011GL047888, l14812, 2011.

Butz, A., Galli, A., Hasekamp, O., Landgraf, J., Tol, P., and Aben, I.: TROPOMI aboard Sentinel-5 Precursor: Prospective performance of CH 4 retrievals for aerosol and cirrus loaded atmospheres, Remote sensing of environment, 120, 267–276, 2012.

Caldeira, K. and Wickett, M. E.: Oceanography: anthropogenic carbon and ocean pH, Nature, 425, 365–365, 2003.

Chevallier, F., Engelen, R. J., and Peylin, P.: The contribution of AIRS data to the estimation of CO2 sources and sinks, Geophysical Research Letters, 32, https://doi.org/10.1029/2005GL024229, 2005.

Chevallier, F., Buchwitz, M., Houweling, S., Aben, I., Palmer, P. I., van Leeuwen, T., and Bergamaschi, P.: ESA Climate Change Initiative (CCI) User Requirements Document (URD) for the Essential Climate Variable (ECV) Greenhouse Gases (GHG), technical note, p. 38, http://www.esa-ghg-cci.org/?q=webfm_send/173, 2014a.

Chevallier, F., Palmer, P. I., Feng, L., Boesch, H., O'Dell, C. W., and Bousquet, P.: Toward robust and consistent regional CO2 flux estimates from in situ and spaceborne measurements of atmospheric CO2, Geophysical Research Letters, 41, 1065–1070, 2014b.

Chédin, A., Hollingsworth, A., Scott, N. A., Serrar, S., Crevoisier, C., and Armante, R.: Annual and seasonal variations of atmospheric CO2, N2O and CO concentrations retrieved from NOAA/TOVS satellite observations, Geophysical Research Letters, 29, 110–1–110–4, https://doi.org/10.1029/2001GL014082, 2002.

Cox, C. and Munk, W.: Statistics of the sea surface derived from sun glitter, Journal of Marine Research, 13, 198–227, 1954.

Cox, P. M., Betts, R. A., Jones, C. D., Spall, S. A., and Totterdell, I. J.: Acceleration of global warming due to carbon-cycle feedbacks in a coupled climate model, Nature, 408, 184–187, 2000.

Crevoisier, C., Chédin, A., Matsueda, H., Machida, T., Armante, R., and Scott, N.: First year of upper tropospheric integrated content of CO2 from IASI hyperspectral infrared observations, Atmospheric Chemistry and Physics, 9, 4797–4810, 2009.

Crisp, D., Atlas, R., Breon, F.-M., Brown, L., Burrows, J., Ciais, P., Connor, B., Doney, S., Fung, I., Jacob, D., Miller, C., O'Brien, D., Pawson, S., Randerson, J., Rayner, P., Salawitch, R., Sander, S., Sen, B., Stephens, G., Tans, P., Toon, G., Wennberg, P., Wofsy, S., Yung, Y., Kuang, Z., Chudasama, B., Sprague, G., Weiss, B., Pollock, R., Kenyon, D., and Schroll, S.: The Orbiting Carbon Observatory (OCO) mission, Advances in Space Research, 34, 700 – 709, https://doi.org/http://doi.org/10.1016/j.asr.2003.08.062, trace Constituents in the Troposphere and Lower Stratosphere, 2004.

Crisp, D., Fisher, B. M., O'Dell, C., Frankenberg, C., Basilio, R., Bösch, H., Brown, L. R., Castano, R., Connor, B., Deutscher, N. M., Eldering, A., Griffith, D., Gunson, M., Kuze, A., Mandrake, L., McDuffie, J., Messerschmidt, J., Miller, C. E., Morino, I., Natraj, V., Notholt, J., O'Brien, D. M., Oyafuso, F., Polonsky, I., Robinson, J., Salawitch, R., Sherlock, V., Smyth, M., Suto, H., Taylor, T. E., Thompson, D. R., Wennberg, P. O., Wunch, D., and Yung, Y. L.: The ACOS CO2 retrieval algorithm Part II: Global XCO2 data characterization, Atmospheric Measurement Techniques, 5, 687–707, https://doi.org/10.5194/amt-5-687-2012, 2012.

Crisp, D., Pollock, H. R., Rosenberg, R., Chapsky, L., Lee, R. A. M., Oyafuso, F. A., Frankenberg, C., O'Dell, C. W., Bruegge, C. J., Doran, G. B., Eldering, A., Fisher, B. M., Fu, D., Gunson, M. R., Mandrake, L., Osterman, G. B., Schwandner, F. M., Sun, K., Taylor, T. E., Wennberg, P. O., and Wunch, D.: The on-orbit performance of the Orbiting Carbon Observatory-2 (OCO-2) instrument and its radiometrically calibrated products, Atmospheric Measurement Techniques, 10, 59–81, https://doi.org/10.5194/amt-10-59-2017, 2017.

De Mazière, M., Sha, M. K., Desmet, F., Hermans, C., Scolas, F., Kumps, N., Metzger, J.-M., Duflot, V., and Cammas, J.-P.: TCCON data from Réunion Island (RE), Release GGG2014.R0, TCCON Data Archive, hosted by CaltechDATA, https://doi.org/10.14291/tccon.ggg2014.reunion01.R0/1149288, 2014.

Detmers, R. G., Hasekamp, O., Aben, I., Houweling, S., van Leeuwen, T. T., Butz, A., Landgraf, J., Köhler, P., Guanter, L., and Poulter, B.: Anomalous carbon uptake in Australia as seen by GOSAT, Geophysical Research Letters, 42, 8177–8184, https://doi.org/10.1002/2015GL065161, http://dx.doi.org/10.1002/2015GL065161, 2015GL065161, 2015.

Deutscher, N. M., Notholt, J., Messerschmidt, J., Weinzierl, C., Warneke, T., Petri, C., Grupe, P., and Katrynski, K.: TCCON data from Bialystok (PL), Release GGG2014.R1, TCCON Data Archive, hosted by CaltechDATA, https://doi.org/10.14291/tccon.ggg2014.bialystok01.R1/1183984, 2015.

Dils, B., Buchwitz, M., Reuter, M., Schneising, O., Boesch, H., Parker, R., Guerlet, S., Aben, I., Blumenstock, T., Burrows, J. P., Butz, A., Deutscher, N. M., Frankenberg, C., Hase, F., Hasekamp, O. P., Heymann, J., De Mazière, M., Notholt, J., Sussmann, R., Warneke, T., Griffith, D., Sherlock, V., and Wunch, D.: The Greenhouse Gas Climate Change Initiative (GHG-CCI): comparative validation of GHG-CCI SCIAMACHY/ENVISAT and TANSO-FTS/GOSAT CO_2 and CH_4 retrieval algorithm products with measurements from the TCCON, Atmospheric Measurement Techniques, 7, 1723–1744, https://doi.org/10.5194/amt-7-1723-2014, http://www.atmos-meas-tech.net/7/1723/2014/, 2014.

Dubovik, O., Sinyuk, A., Lapyonok, T., Holben, B. N., Mishchenko, M., Yang, P., Eck, T. F., Volten, H., Munoz, O., Veihelmann, B., et al.: Application of spheroid models to account for aerosol particle nonsphericity in remote sensing of desert dust, Journal of Geophysical Research: Atmospheres, 111, 2006.

Eldering, A., O'Dell, C. W., Wennberg, P. O., Crisp, D., Gunson, M. R., Viatte, C., Avis, C., Braverman, A., Castano, R., Chang, A., Chapsky, L., Cheng, C., Connor, B., Dang, L., Doran, G., Fisher, B., Frankenberg, C., Fu, D., Granat, R., Hobbs, J., Lee, R. A. M., Mandrake, L., McDuffie, J., Miller, C. E., Myers, V., Natraj, V., O'Brien, D., Osterman, G. B., Oyafuso, F., Payne, V. H., Pollock, H. R., Polonsky, I., Roehl, C. M., Rosenberg, R., Schwandner, F., Smyth, M., Tang, V., Taylor, T. E., To, C., Wunch, D., and Yoshimizu, J.: The Orbiting Carbon Observatory-2: first 18 months of science data products, Atmospheric Measurement Techniques, 10, 549–563, https://doi.org/10.5194/amt-10-549-2017, http://www.atmos-meas-tech.net/10/549/2017/, 2017.

Engelen, R. J., Andersson, E., Chevallier, F., Hollingsworth, A., Matricardi, M., McNally, A. P., Thépaut, J.-N., and Watts, P. D.: Estimating atmospheric CO2 from advanced infrared satellite radiances within an operational 4D-Var data assimilation system: Methodology and first results, Journal of Geophysical Research: Atmospheres, 109, 2004.

Farr, T. G., Rosen, P. A., Caro, E., Crippen, R., Duren, R., Hensley, S., Kobrick, M., Paller, M., Rodriguez, E., Roth, L., et al.: The shuttle radar topography mission, Reviews of geophysics, 45, 2007.

Feist, D. G., Arnold, S. G., John, N., and Geibel, M. C.: TCCON data from Ascension Island (SH), Release GGG2014.R0, TCCON Data Archive, hosted by CaltechDATA, https://doi.org/10.14291/tccon.ggg2014.ascension01.R0/1149285, 2014.

Goo, T.-Y., Oh, Y.-S., and Velazco, V. A.: TCCON data from Anmeyondo (KR), Release GGG2014.R0, TCCON Data Archive, hosted by CaltechDATA, https://doi.org/10.14291/tccon.ggg2014.anmeyondo01.R0/1149284, 2014.

Griffith, D. W. T., Deutscher, N. M., Velazco, V. A., Wennberg, P. O., Yavin, Y., Keppel-Aleks, G., Washenfelder, R., Toon, G. C., Blavier, J.-F., Paton-Walsh, C., Jones, N. B., Kettlewell, G. C., Connor, B., Macatangay, R. C., Roehl, C., Ryczek, M., Glowacki, J., Culgan, T., and Bryant, G.: TCCON data from Darwin (AU), Release GGG2014.R0, TCCON Data Archive, hosted by CaltechDATA, https://doi.org/10.14291/tccon.ggg2014.darwin01.R0/1149290, 2014a.

Griffith, D. W. T., Velazco, V. A., Deutscher, N. M., Paton-Walsh, C., Jones, N. B., Wilson, S. R., Macatangay, R. C., Kettlewell, G. C., Buchholz, R. R., and Riggenbach, M.: TCCON data from Wollongong (AU), Release GGG2014.R0, TCCON Data Archive, hosted by CaltechDATA, https://doi.org/10.14291/tccon.ggg2014.wollongong01.R0/1149291, 2014b.

Guerlet, S., Basu, S., Butz, A., Krol, M., Hahne, P., Houweling, S., Hasekamp, O. P., and Aben, I.: Reduced carbon uptake during the 2010 Northern Hemisphere summer from GOSAT, Geophysical Research Letters, 40, 2378–2383, https://doi.org/10.1002/grl.50402, http://dx.doi.org/10.1002/grl.50402, 2013a.

Guerlet, S., Butz, A., Schepers, D., Basu, S., Hasekamp, O. P., Kuze, A., Yokota, T., Blavier, J.-F., Deutscher, N. M., Griffith, D. W., Hase, F., Kyro, E., Morino, I., Sherlock, V., Sussmann, R., Galli, A., and Aben, I.: Impact of aerosol and thin cirrus on retrieving and validating XCO2 from GOSAT shortwave infrared measurements, Journal of Geophysical Research: Atmospheres, 118, 4887–4905, https://doi.org/10.1002/jgrd.50332, 2013b.

Gurney, K. R., Law, R. M., Denning, A. S., Rayner, P. J., Baker, D., Bousquet, P., Bruhwiler, L., Chen, Y.-H., Ciais, P., Fan, S., et al.: Towards robust regional estimates of CO2 sources and sinks using atmospheric transport models, Nature, 415, 626–630, 2002.

Hase, F., Blumenstock, T., Dohe, S., Gross, J., and Kiel, M.: TCCON data from Karlsruhe (DE), Release GGG2014.R1, TCCON Data Archive, hosted by CaltechDATA, https://doi.org/10.14291/tccon.ggg2014.karlsruhe01.R1/1182416, 2015.

Hasekamp, O. P. and Butz, A.: Efficient calculation of intensity and polarization spectra in vertically inhomogeneous scattering and absorbing atmospheres, Journal of Geophysical Research: Atmospheres, 113, n/a–n/a, https://doi.org/10.1029/2008JD010379, d20309, 2008.

Hasekamp, O. P. and Landgraf, J.: A linearized vector radiative transfer model for atmospheric trace gas retrieval, Journal of Quantitative Spectroscopy and Radiative Transfer, 75, 221–238, 2002.

Hasekamp, O. P. and Landgraf, J.: Linearization of vector radiative transfer with respect to aerosol properties and its use in satellite remote sensing, Journal of Geophysical Research: Atmospheres (1984–2012), 110, https://doi.org/10.1029/2004JD005260, 2005a.

Hasekamp, O. P. and Landgraf, J.: Retrieval of aerosol properties over the ocean from multispectral single-viewing-angle measurements of intensity and polarization: Retrieval approach, information content, and sensitivity study, Journal of Geophysical Research: Atmospheres, 110, 2005b.

Hönninger, G., Friedeburg, C. v., and Platt, U.: Multi axis differential optical absorption spectroscopy (MAX-DOAS), Atmospheric Chemistry and Physics, 4, 231–254, 2004.

Houweling, S., Breon, F.-M., Aben, I., Rödenbeck, C., Gloor, M., Heimann, M., and Ciais, P.: Inverse modeling of CO 2 sources and sinks using satellite data: a synthetic inter-comparison of measurement techniques and their performance as a function of space and time, Atmospheric Chemistry and Physics, 4, 523–538, 2004.

Houweling, S., Aben, I., Breon, F.-M., Chevallier, F., Deutscher, N., Engelen, R., Gerbig, C., Griffith, D., Hungershoefer, K., Macatangay, R., et al.: The importance of transport model uncertainties for the estimation of CO 2 sources and sinks using satellite measurements, Atmospheric chemistry and physics, 10, 9981–9992, 2010.

Houweling, S., Krol, M., Bergamaschi, P., Frankenberg, C., Dlugokencky, E. J., Morino, I., Notholt, J., Sherlock, V., Wunch, D., Beck, V., Gerbig, C., Chen, H., Kort, E. A., Röckmann, T., and Aben, I.: A multi-year methane inversion using SCIAMACHY, accounting for systematic errors using TCCON measurements, Atmospheric Chemistry and Physics, 14, 3991–4012, https://doi.org/10.5194/acp-14-3991-2014, 2014.

Iraci, L. T., Podolske, J., Hillyard, P. W., Roehl, C., Wennberg, P. O., Blavier, J.-F., Allen, N., Wunch, D., Osterman, G., and Albertson, R.: TCCON data from Edwards (US), Release GGG2014.R1, TCCON Data Archive, hosted by CaltechDATA, https://doi.org/10.14291/tccon.ggg2014.edwards01.R1/1255068, 2016.

Jung, Y., Kim, J., Kim, W., Boesch, H., Lee, H., Cho, C., and Goo, T.-Y.: Impact of aerosol property on the accuracy of a CO2 retrieval algorithm from satellite remote sensing, Remote Sensing, 8, 322, 2016.

Kawakami, S., Ohyama, H., Arai, K., Okumura, H., Taura, C., Fukamachi, T., and Sakashita, M.: TCCON data from Saga (JP), Release GGG2014.R0, TCCON Data Archive, hosted by CaltechDATA, https://doi.org/10.14291/tccon.ggg2014.saga01.R0/1149283, 2014.

Kivi, R., Heikkinen, P., and Kyrö, E.: TCCON data from Sodankylä (FI), Release GGG2014.R0, TCCON Data Archive, hosted by CaltechDATA, https://doi.org/10.14291/tccon.ggg2014.sodankyla01.R0/1149280, 2014.

Kulawik, S., Wunch, D., O'Dell, C., Frankenberg, C., Reuter, M., Oda, T., Chevallier, F., Sherlock, V., Buchwitz, M., Osterman, G., Miller, C. E., Wennberg, P. O., Griffith, D., Morino, I., Dubey, M. K., Deutscher, N. M., Notholt, J., Hase, F., Warneke, T., Sussmann, R., Robinson, J., Strong, K., Schneider, M., De Mazière, M., Shiomi, K., Feist, D. G., Iraci, L. T., and Wolf, J.: Consistent evaluation of ACOS-GOSAT, BESD-SCIAMACHY, CarbonTracker, and MACC through comparisons to TCCON, Atmospheric Measurement Techniques, 9, 683–709, https://doi.org/10.5194/amt-9-683-2016, https://www.atmos-meas-tech.net/9/683/2016/, 2016.

Kulawik, S. S., O'Dell, C., Payne, V. H., Kuai, L., Worden, H. M., Biraud, S. C., Sweeney, C., Stephens, B., Iraci, L. T., Yates, E. L., and Tanaka, T.: Lower-tropospheric CO_2 from near-infrared ACOS-GOSAT observations, Atmospheric Chemistry and Physics, 17, 5407–5438, https://doi.org/10.5194/acp-17-5407-2017, 2017.

Lamouroux, J., Tran, H., Laraia, A., Gamache, R., Rothman, L., Gordon, I., and Hartmann, J.-M.: Updated database plus software for line-mixing in CO 2 infrared spectra and their test using laboratory spectra in the 1.5–2.3 μm region, Journal of Quantitative Spectroscopy and Radiative Transfer, 111, 2321–2331, 2010.

Mandrake, L., O'Dell, C., Wunch, D., Wennberg, P., Fisher, B., Osterman, G., and Eldering, A.: Orbiting Carbon Observatory-2 (OCO-2) Warn Level, Bias Correction, and Lite File Product Description, Tech. rep., Tech. rep., Jet Propulsion Laboratory, California Institute of Technology, Pasasdena, available at: http://disc. sci. gsfc. nasa. gov/OCO-2/documentation/oco-2-v7/OCO2_XCO2_Lite_Files_and_Bias_Correction_0915_sm. pdf (last access: 16 October 2015), 2015.

Morino, I., Matsuzaki, T., and Horikawa, M.: TCCON data from Tsukuba (JP), 125HR, Release GGG2014.R1, TCCON Data Archive, hosted by CaltechDATA, https://doi.org/10.14291/tccon.ggg2014.tsukuba02.R1/1241486, 2016a.

Morino, I., Yokozeki, N., Matsuzaki, T., and Horikawa, M.: TCCON data from Rikubetsu (JP), Release GGG2014.R1, TCCON Data Archive, hosted by CaltechDATA, https://doi.org/10.14291/tccon.ggg2014.rikubetsu01.R1/1242265, 2016b.

Notholt, J., Petri, C., Warneke, T., Deutscher, N. M., Buschmann, M., Weinzierl, C., Macatangay, R. C., and Grupe, P.: TCCON data from Bremen (DE), Release GGG2014.R0, TCCON Data Archive, hosted by CaltechDATA, https://doi.org/10.14291/tccon.ggg2014.bremen01.R0/1149275, 2014.

O'Dell, C. W., Connor, B., Bösch, H., O'Brien, D., Frankenberg, C., Castano, R., Christi, M., Eldering, D., Fisher, B., Gunson, M., McDuffie, J., Miller, C. E., Natraj, V., Oyafuso, F., Polonsky, I., Smyth, M., Taylor, T., Toon, G. C., Wennberg, P. O., and Wunch, D.: The ACOS CO_2 retrieval algorithm Part 1: Description and validation against synthetic observations, Atmospheric Measurement Techniques, 5, 99–121, https://doi.org/10.5194/amt-5-99-2012, 2012.

Patra, P. K., Maksyutov, S., Sasano, Y., Nakajima, H., Inoue, G., and Nakazawa, T.: An evaluation of CO2 observations with Solar Occultation FTS for Inclined-Orbit Satellite sensor for surface source inversion, Journal of Geophysical Research: Atmospheres, 108, 2003.

Peters, W., Jacobson, A. R., Sweeney, C., Andrews, A. E., Conway, T. J., Masarie, K., Miller, J. B., Bruhwiler, L. M. P., Pétron, G., Hirsch, A. I., Worthy, D. E. J., van der Werf, G. R., Randerson, J. T., Wennberg, P. O., Krol, M. C., and Tans, P. P.: An atmospheric perspective on North American carbon dioxide exchange: CarbonTracker, Proceedings of the National Academy of Sciences, 104, 18 925–18 930, https://doi.org/10.1073/pnas.0708986104, 2007.

Phillips, D. L.: A technique for the numerical solution of certain integral equations of the first kind, Journal of the ACM (JACM), 9, 84–97, 1962.

Prentice, I. C., Farquhar, G., Fasham, M., Goulden, M., Heimann, M., Jaramillo, V., Kheshgi, H., LeQuéré, C., Scholes, R., and Wallace, D. W.: The carbon cycle and atmospheric carbon dioxide, Cambridge University Press, 2001.

Rayner, P. and O'Brien, D.: The utility of remotely sensed CO2 concentration data in surface source inversions, Geophysical research letters, 28, 175–178, 2001.

Reuter, M., Buchwitz, M., Schneising, O., Heymann, J., Bovensmann, H., and Burrows, J.: A method for improved SCIAMACHY CO 2 retrieval in the presence of optically thin clouds, Atmospheric Measurement Techniques, 3, 209–232, 2010.

Reuter, M., Bovensmann, H., Buchwitz, M., Burrows, J. P., Connor, B. J., Deutscher, N. M., Griffith, D. W. T., Heymann, J., Keppel-Aleks, G., Messerschmidt, J., Notholt, J., Petri, C., Robinson, J., Schneising, O., Sherlock, V., Velazco, V., Warneke, T., Wennberg, P. O., and Wunch, D.: Retrieval of atmospheric CO2 with enhanced accuracy and precision from SCIAMACHY: Validation with FTS measurements and comparison with model results, Journal of Geophysical Research: Atmospheres, 116, n/a–n/a, https://doi.org/10.1029/2010JD015047, d04301, 2011.

Rodgers, C. D.: Inverse methods for atmospheric sounding: theory and practice, vol. 2, World scientific, 2000.

Rothman, L. S., Gordon, I. E., Barbe, A., Benner, D. C., Bernath, P. F., Birk, M., Boudon, V., Brown, L. R., Campargue, A., Champion, J.-P., et al.: The HITRAN 2008 molecular spectroscopic database, Journal of Quantitative Spectroscopy and Radiative Transfer, 110, 533–572, 2009.

Schepers, D., Guerlet, S., Butz, A., Landgraf, J., Frankenberg, C., Hasekamp, O., Blavier, J.-F., Deutscher, N., Griffith, D., Hase, F., et al.: Methane retrievals from Greenhouse Gases Observing Satellite (GOSAT) shortwave infrared measurements: Performance comparison of proxy and physics retrieval algorithms, Journal of Geophysical Research: Atmospheres, 117, 2012.

Schepers, D., aan de Brugh, J., Hahne, P., Butz, A., Hasekamp, O., and Landgraf, J.: LINTRAN v2. 0: A linearised vector radiative transfer model for efficient simulation of satellite-born nadir-viewing reflection measurements of cloudy atmospheres, Journal of Quantitative Spectroscopy and Radiative Transfer, 149, 347–359, 2014.

Sherlock, V., Connor, B., Robinson, J., Shiona, H., Smale, D., and Pollard, D.: TCCON data from Lauder (NZ), 125HR, Release GGG2014.R0, TCCON Data Archive, hosted by CaltechDATA, https://doi.org/10.14291/tccon.ggg2014.lauder02.R0/1149298, 2014.

Sussmann, R. and Rettinger, M.: TCCON data from Garmisch (DE), Release GGG2014.R0, TCCON Data Archive, hosted by CaltechDATA, https://doi.org/10.14291/tccon.ggg2014.garmisch01.R0/1149299, 2014.

Taylor, T. E., O'Dell, C. W., Frankenberg, C., Partain, P. T., Cronk, H. Q., Savtchenko, A., Nelson, R. R., Rosenthal, E. J., Chang, A. Y., Fisher, B., Osterman, G. B., Pollock, R. H., Crisp, D., Eldering, A., and Gunson, M. R.: Orbiting Carbon Observatory-2 (OCO-2) cloud screening algorithms: validation against collocated MODIS and CALIOP data, Atmospheric Measurement Techniques, 9, 973–989, https://doi.org/10.5194/amt-9-973-2016, 2016.

Te, Y., Jeseck, P., and Janssen, C.: TCCON data from Paris (FR), Release GGG2014.R0, TCCON Data Archive, hosted by CaltechDATA, https://doi.org/10.14291/tccon.ggg2014.paris01.R0/1149279, 2014.

Tikhonov, A. N.: Solution of incorrectly formulated problems and the regularization method, in: Doklady Akademii Nauk SSSR, vol. 151, pp. 501–504, 1963.

Tran, H. and Hartmann, J.-M.: An improved O2 A band absorption model and its consequences for retrievals of photon paths and surface pressures, Journal of Geophysical Research: Atmospheres, 113, https://doi.org/10.1029/2008JD010011, d18104, 2008.

Warneke, T., Messerschmidt, J., Notholt, J., Weinzierl, C., Deutscher, N. M., Petri, C., Grupe, P., Vuillemin, C., Truong, F., Schmidt, M., Ramonet, M., and Parmentier, E.: TCCON data from Orléans (FR), Release GGG2014.R0, TCCON Data Archive, hosted by CaltechDATA, https://doi.org/10.14291/tccon.ggg2014.orleans01.R0/1149276, 2014.

Wennberg, P. O., Roehl, C., Wunch, D., Toon, G. C., Blavier, J.-F., Washenfelder, R., Keppel-Aleks, G., Allen, N., and Ayers, J.: TCCON data from Park Falls (US), Release GGG2014.R0, TCCON Data Archive, hosted by CaltechDATA, https://doi.org/10.14291/tccon.ggg2014.parkfalls01.R0/1149161, 2014.

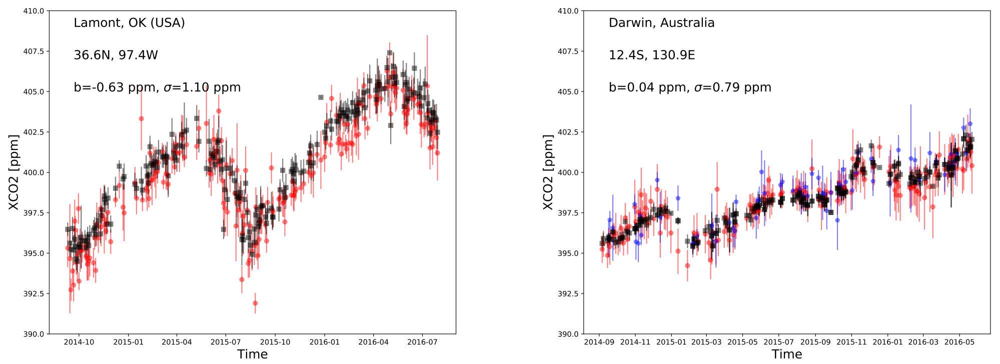

Figure 1. Time variation of X_{CO_2} retrievals from OCO-2 observations over land (red dots) and ocean (blue pentagon) and collocated TCCON measurements (black square) for Lamont and Darwin stations. Standard deviation of individual TCCON measurement and satellite retrievals are presented with the length of bar. In each subplot, the mean bias (b) and standard deviation(σ) of the difference between RemoTeC/OCO-2 retrievals and TCCON measurements and site location in latitude and longitude are included. The shown results here are bias-corrected data.

Wennberg, P. O., Wunch, D., Roehl, C., Blavier, J.-F., Toon, G. C., and Allen, N.: TCCON data from Lamont (US), Release GGG2014.R1, TCCON Data Archive, hosted by CaltechDATA, https://doi.org/10.14291/tccon.ggg2014.lamont01.R1/1255070, 2016.

Wunch, D., Toon, G. C., Blavier, J.-F. L., Washenfelder, R. A., Notholt, J., Connor, B. J., Griffith, D. W., Sherlock, V., and Wennberg, P. O.: The total carbon column observing network, Philosophical Transactions of the Royal Society of London A: Mathematical, Physical and Engineering Sciences, 369, 2087–2112, 2011a.

Wunch, D., Wennberg, P., Toon, G., Connor, B., Fisher, B., Osterman, G., Frankenberg, C., Mandrake, L., O'Dell, C., Ahonen, P., et al.: A method for evaluating bias in global measurements of CO 2 total columns from space, Atmospheric Chemistry and Physics, 11, 12 317–12 337, 2011b.

Wunch, D., Toon, G. C., Sherlock, V., Deutscher, N. M., Liu, C., Feist, D. G., and Wennberg, P. O.: The Total Carbon Column Observing Network's GGG2014 Data Version, Carbon Dioxide Information Analysis Center, Oak Ridge National Laboratory, Oak Ridge, Tennessee, USA, available at: doi, 10, https://doi.org/10.14291/tccon.ggg2014.documentation.R0/1221662, 2015.

Wunch, D., Wennberg, P. O., Osterman, G., Fisher, B., Naylor, B., Roehl, C. M., O'Dell, C., Mandrake, L., Viatte, C., Kiel, M., Griffith, D. W. T., Deutscher, N. M., Velazco, V. A., Notholt, J., Warneke, T., Petri, C., De Maziere, M., Sha, M. K., Sussmann, R., Rettinger, M., Pollard, D., Robinson, J., Morino, I., Uchino, O., Hase, F., Blumenstock, T., Feist, D. G., Arnold, S. G., Strong, K., Mendonca, J., Kivi, R., Heikkinen, P., Iraci, L., Podolske, J., Hillyard, P. W., Kawakami, S., Dubey, M. K., Parker, H. A., Sepulveda, E., García, O. E., Te, Y., Jeseck, P., Gunson, M. R., Crisp, D., and Eldering, A.: Comparisons of the Orbiting Carbon Observatory-2 (OCO-2) X_{CO_2} measurements with TCCON, Atmospheric Measurement Techniques, 10, 2209–2238, https://doi.org/10.5194/amt-10-2209-2017, 2017.

Yokota, T., Yoshida, Y., Eguchi, N., Ota, Y., Tanaka, T., Watanabe, H., and Maksyutov, S.: Global concentrations of CO2 and CH4 retrieved from GOSAT: First preliminary results, Sola, 5, 160–163, 2009.

Yoshida, Y., Ota, Y., Eguchi, N., Kikuchi, N., Nobuta, K., Tran, H., Morino, I., and Yokota, T.: Retrieval algorithm for CO_2 and CH_4 column abundances from short-wavelength infrared spectral observations by the Greenhouse gases observing satellite, Atmospheric Measurement Techniques, 4, 717–734, https://doi.org/10.5194/amt-4-717-2011, http://www.atmos-meas-tech.net/4/717/2011/, 2011.

Table 1. State vector elements and their prior values considered in the retrieval.

state vector element	a prior	unit
twelve CO_2 sub-columns	CarbonTracker 2013	molec cm^{-2}
H_2O total column	ECMWF	molec cm^{-2}
CH_4 total columns	TM5	molec cm^{-2}
three parameters of the Lambertian surface albedo, NIR	estimated from mean radiance	-
addictive intensity offset, NIR	0.0	Ph sec^{-1} m^{-2} sr^{-1} μm^{-1}
zero order spectral shift, NIR	0.0	-
solar reference spectral shift, NIR	0.0	-
three parameters of the Lambertian surface albedo, SWIR1	estimated from mean radiance	-
addictive intensity offset, SWIR1	0.0	Ph sec^{-1} m^{-2} sr^{-1} μm^{-1}
zero order spectral shift, SWIR1	0.0	-
solar reference spectral shift, SWIR1	0.0	-
three parameters of the Lambertian surface albedo, SWIR2	estimated from mean radiance	-
addictive intensity offset, SWIR2	0.0	Ph sec^{-1} m^{-2} sr^{-1} μm^{-1}
zero order spectral shift, SWIR2	0.0	-
solar reference spectral shift, SWIR2	0.0	-
aerosol size parameter	4.5	μm
aerosol column	6.84×10^{12}	m^{-2}
aerosol layer central height	3000	m

Table 2. Settings of the filters used for excluding RemoTeC/OCO-2 X_{CO_2} retrievals. The sign '-' indicates using the same option as in land retrievals.

Parameter	Definition	Allowed Range	
		Land	Ocean
sza	Solar zenith angle	val$\leq 70°$	-
vza	Viewing zenith angle	val$\leq 45°$	-
iter	Number of retrieval iterations	val≤ 30	-
dfs	Degrees of Freedom for Signal for CO_2	val≥ 1.0	-
χ^2	Overall ~~fit residuals~~goodness of fit	val≤ 7.0	-
χ^2_{1st}	~~Fit residuals~~ Goodness of fit in O_2 A-band	val≤ 7.0	-
Blended albedo*	2.4×albedo_NIR - 1.13×albedo_SWIR-2	val≤ 0.9	None
alb_2	Added Lambertian term in SWIR-2 band	None	val≤ 0.065
sev	Surface elevation variation	val≤ 75 m	None
α_s	Aerosol size parameter	$3.5 \leq$val≤ 8.0	$3.5 \leq$val≤ 5.5
$\tau_{0.765}$	Aerosol optical depth in O_2 A-band	val≤ 0.35	val≤ 0.55
Aerosol ratio parameter	$\tau_{0.765} * z_s/\alpha_s$, z_s is aerosol layer height	val≤ 300 m	-
Xerr	Retrieval uncertainty for X_{CO_2}	val≤ 2.0 ppm	-
$Ioff_1$	Fitted Intensity offset ratio in NIR band	$-0.005 \leq$val≤ 0.015	-
$Ioff_2$	Fitted Intensity offset ratio in SWIR-1 band	$-0.001 \leq$val≤ 0.015	-
$Ioff_3$	Fitted Intensity offset ratio in SWIR-2 band	$-0.001 \leq$val≤ 0.015	-

*The blended albedo filter was first introduced in Wunch et al. (2011b).

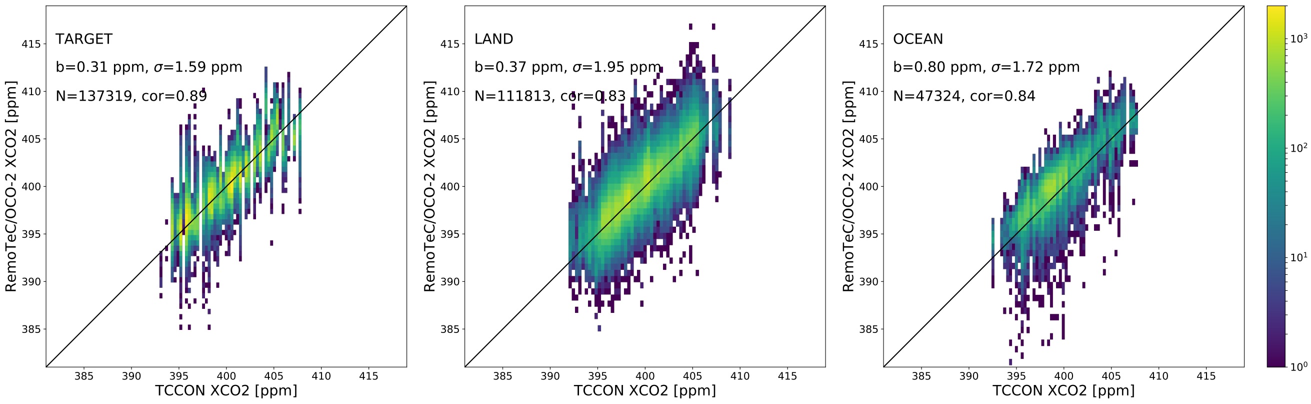

Figure 2. Validation of individual X_{CO_2} retrieved from OCO-2 measurements with collocated TCCON data before bias correction. Here, target retrievals are separated intentionally from land retrievals results which thus only include measurements obtained under nadir and glint modes. Ocean retrievals only include glint mode observations over ocean. For retrievals collocated with multiple TCCON stations, we use data from the closest station. The bias (b), sounding precision (σ), number of points (N), the Pearson correlation coefficient (cor) and one-to-one line are included. Different colors represent the frequency of point occurrence.

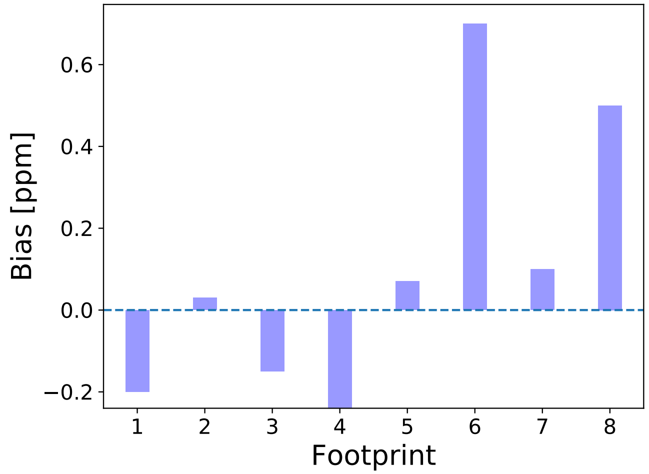

Figure 3. Estimated swath-dependent biases using Target mode observations.

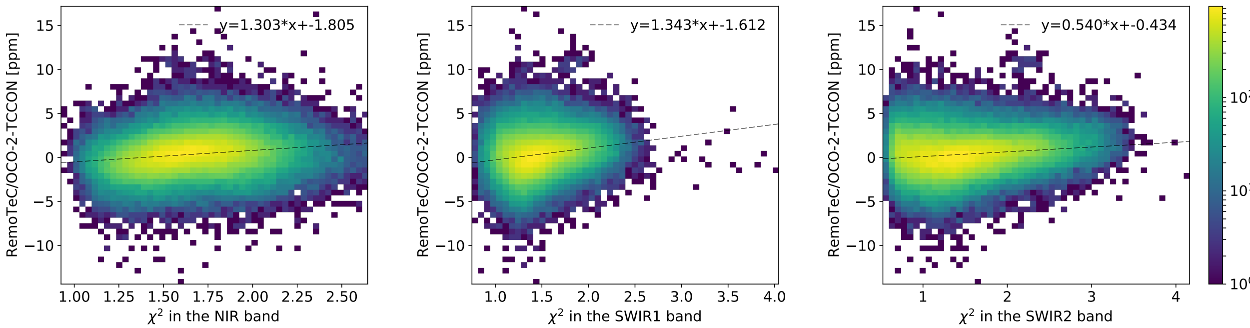

Figure 4. Error on X_{CO_2} retrievals as a function of the goodness of fit ~~resudual~~ in the NIR, SWIR-1 ~~band~~and SWIR2 bands. Different colors represent the frequency of point occurrence. The dashed line is a linear regression fit to the data.

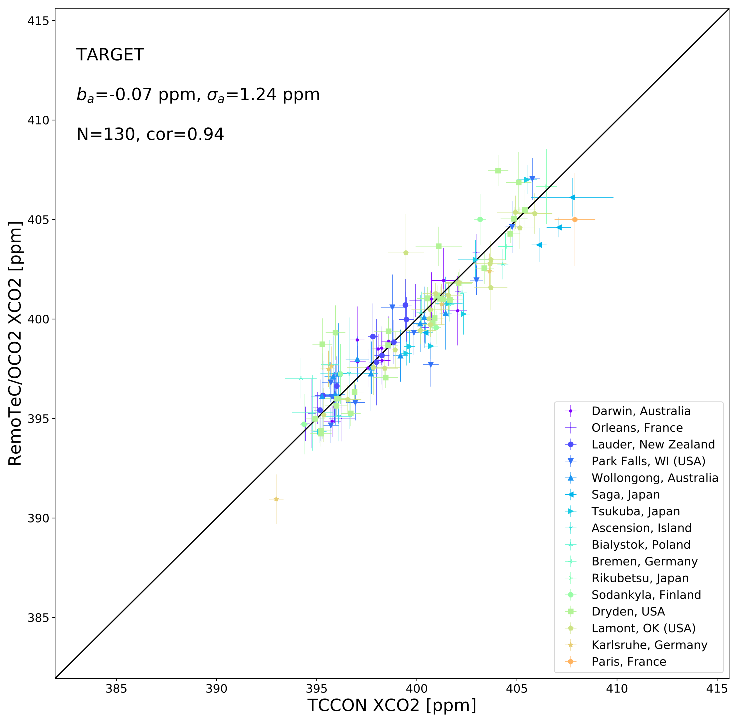

Figure 5. Validation of averaged X_{CO_2} retrieved from OCO-2 target measurements with collocated TCCON data. The retrieval results shown here are overpass averages of single soundings per station within 2 hours. The standard deviation of individual TCCON data and that of RemoTeC/OCO-2 retrievals are presented with error bars. The bias (b_a), standard deviation (σ_a), number of points (N), the Pearson correlation coefficient (cor) and one-to-one line are included.

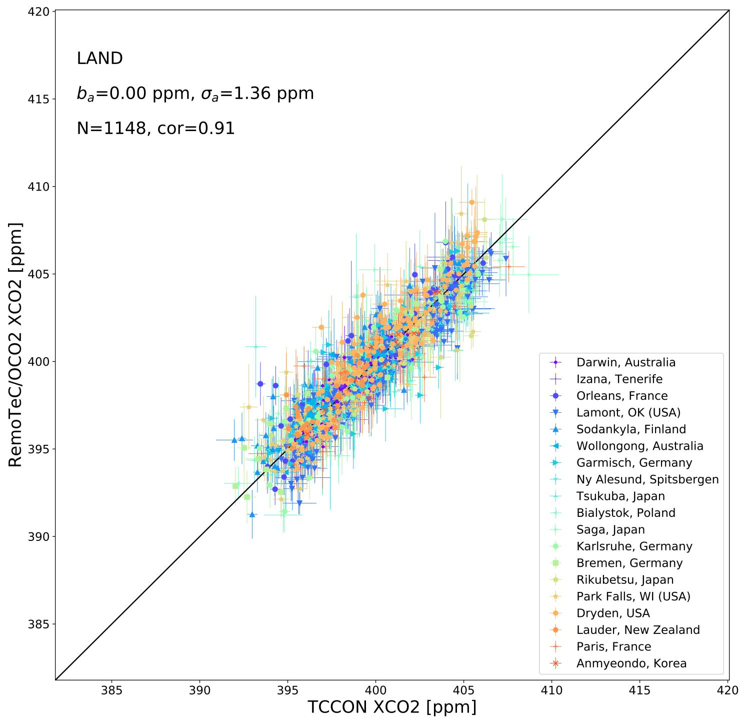

Figure 6. Same as Fig. 5, but for OCO-2 land type measurements obtained under nadir and glint modes.

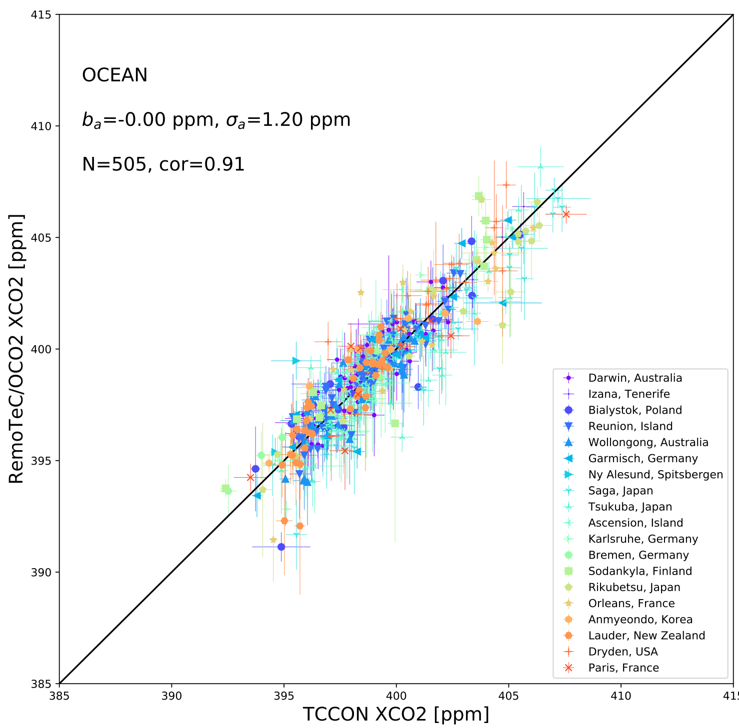

Figure 7. Same as Fig. 5, but for OCO-2 ocean type measurements obtained under glint mode.

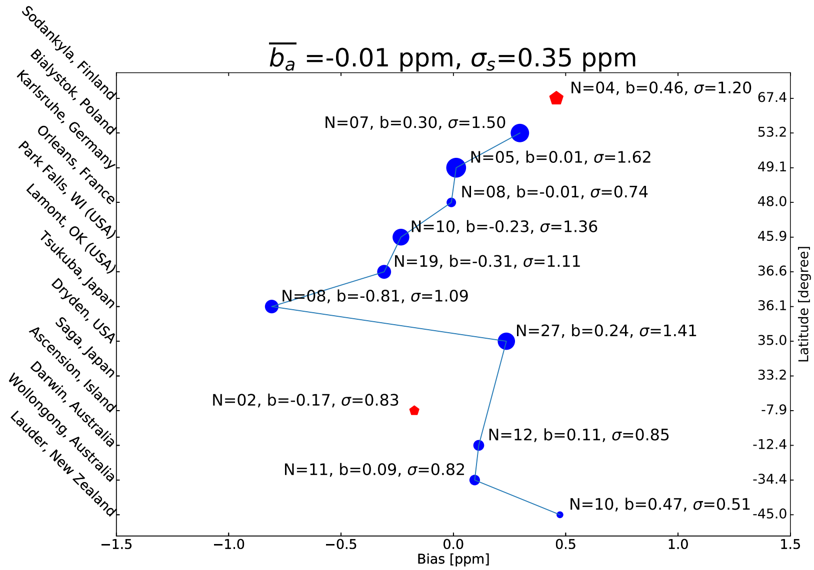

Figure 8. The dependence of the bias between RemoTeC/OCO-2 target X_{CO_2} retrievals coincident with TCCON data on the latitude of each station. Shown are the averaged results for bias-corrected X_{CO_2} retrievals. Stations with less than 5 collocation points (marked with red pentagon) should be interpreted with care and are therefore excluded from the calculation of the derived parameters including mean bias ($\overline{b_a}$) and the station-to-station variability (σ_s). For each station, number of valid points (N), bias (b) and standard deviation (σ) are listed next to the dot point. The ~~length~~ size of each ~~bar~~ dot represents the standard deviation of the difference at each station.

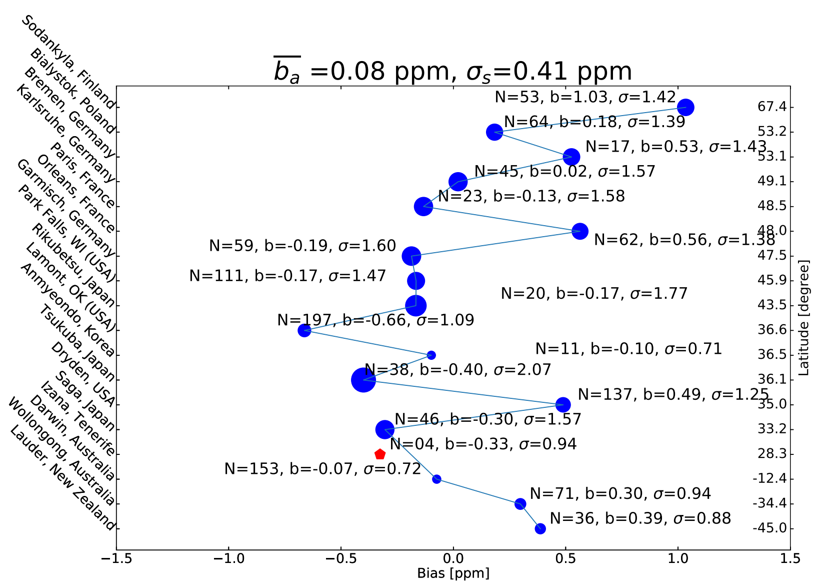

Figure 9. Same as Fig. 8, but for OCO-2 land type measurements obtained under nadir and glint modes.

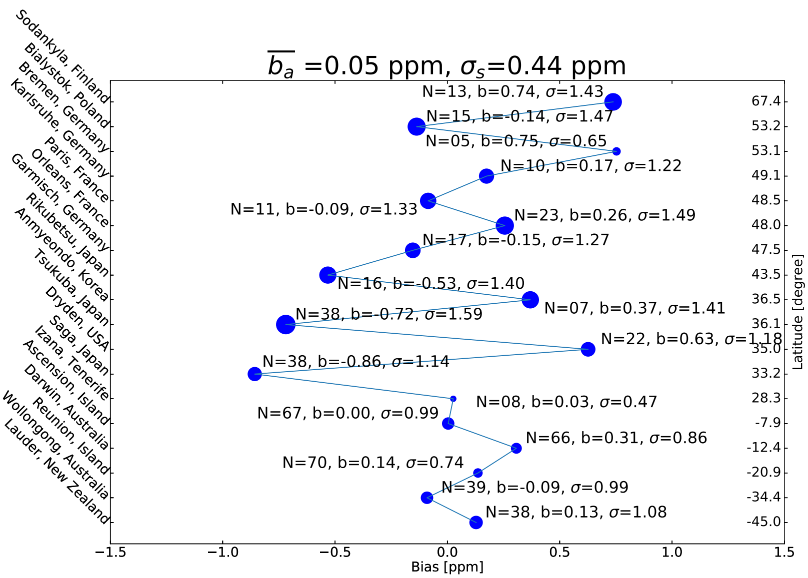

Figure 10. Same as Fig. 8, but for OCO-2 ocean type measurements obtained under glint mode.

Table 3. Bias between X_{CO_2} retrieval from RemoTeC/OCO-2, including target, land and ocean retrievals, and TCCON data at individual stations in four different time intervals of a calendar year (Q1:1 January-31 March, Q2:1 April-30 June, Q3:1 July-30 September, Q4:1 October-31 December). For each time interval, we only use data from stations with more than 5 collocated points. In each table cell, bias, standard deviation and number of points are included and those with larger standard error ($\sigma/\sqrt{N} > 0.5$ ppm) after bias correction will also be neglected as done by Dils et al. (2014). For stations with all four seasonal biases, the standard deviation of these four biases ("Seas") are also caculated. This parameter is an indicator of their seaonal variability.

Stations	Q1	Q2	Q3	Q4	Seas	Reference
Sodankyla, Finland (67.3N, 26.6E)	-	0.70(1.49, 39)	1.18(1.28, 30)	-	-	Kivi et al. (2014)
Bialystok, Poland (53.2N, 23.0E)	-0.34(1.34, 14)	0.02(1.31, 40)	0.62(1.60, 25)	0.02(0.93, 7)	0.34	Deutscher et al. (2015)
Bremen, Germany (53.1N, 8.8E)	-	-0.04(0.95, 7)	1.04(1.20, 14)	-	-	Notholt et al. (2014)
Karlsruhe, Germany (49.1N, 8.4E)	-	-0.16(1.37, 25)	0.09(1.75, 24)	0.59(0.75, 6)	-	Hase et al. (2015)
Park Falls, WI(USA) (48.4N, 2.3E)	-0.14(1.16, 17)	-0.37(1.53, 38)	0.10(1.52, 46)	-0.44(1.27, 20)	0.21	Wennberg et al. (2014)
Paris, France (48.4N, 2.3E)	-	-0.15(1.10, 11)	0.33(1.44, 19)	-	-	Te et al. (2014)
Izana, Tenerife (48.4N, 2.3E)	-0.24(0.73, 7)	-	-	-	-	Blumenstock et al. (2014)
Orleans, France (47.9N, 2.1E)	0.36(1.01, 19)	0.34(1.04, 34)	0.32(1.81, 25)	0.98(1.47, 15)	0.28	Warneke et al. (2014)
Garmisch, Germany (47.4N, 11.0E)	-0.04(1.47, 15)	-0.49(1.56, 28)	0.02(1.34, 23)	-	-	Sussmann and Rettinger (2014)
Rikubetsu, Japan(43.4N, 143.7E)	-1.21(1.64, 11)	-0.13(1.64, 13)	0.81(1.03, 6)	-0.24(1.04, 7)	0.71	Morino et al. (2016b)
Lamont, OK(USA) (36.6N, 97.4W)	-0.71(1.06, 55)	-0.35(1.01, 53)	-0.51(1.29, 59)	-1.00(0.83, 49)	0.24	Wennberg et al. (2016)
Anmyeondo, Korea (36.5N, 126.3E)	-0.26(0.58, 5)	-	0.67(0.85, 7)	-	-	Goo et al. (2014)
Tsukuba, Japan (36.0N, 140.1E)	-1.31(1.18, 26)	0.07(1.17, 12)	-	-1.00(1.17, 29)	-	Morino et al. (2016a)
Dryden, USA (34.9N, 117.8W)	0.10(1.08, 40)	0.85(0.99, 59)	0.55(1.56, 48)	0.16(1.24, 39)	0.30	Iraci et al. (2016)
Saga, Japan (33.2N, 130.2E)	-1.24(0.80, 14)	-0.93(1.05, 27)	-0.32(1.86, 24)	-0.19(1.33, 23)	0.43	Kawakami et al. (2014)
Ascension, Island (7.9165S, 14.3325W)	0.19(1.03, 12)	0.07(0.92, 18)	-0.04(0.99, 14)	-0.12(0.99, 23)	0.12	Feist et al. (2014)
Darwin, Australia (12.4S, 130.9E)	-0.21(0.88, 55)	0.01(0.71, 61)	0.38(0.58, 49)	0.04(0.81, 66)	0.21	Griffith et al. (2014a)
Reunion, Island (20.901S, 55.485E)	0.10(0.69, 9)	-0.23(0.75, 17)	0.12(0.61, 25)	0.50(0.73, 19)	0.26	De Mazière et al. (2014)
Wollongong, Australia (34.4S, 150.8E)	0.04(0.98, 41)	0.26(0.93, 17)	0.21(1.18, 26)	0.19(0.76, 37)	0.08	Griffith et al. (2014b)
Lauder, New Zealand (45.0S, 169.6E)	0.19(0.99, 29)	0.53(0.67, 10)	0.13(0.92, 8)	0.31(0.97, 37)	0.15	Sherlock et al. (2014)
ALL	0.52	0.42	0.43	0.54	-	
SRA		SRA=0.52				

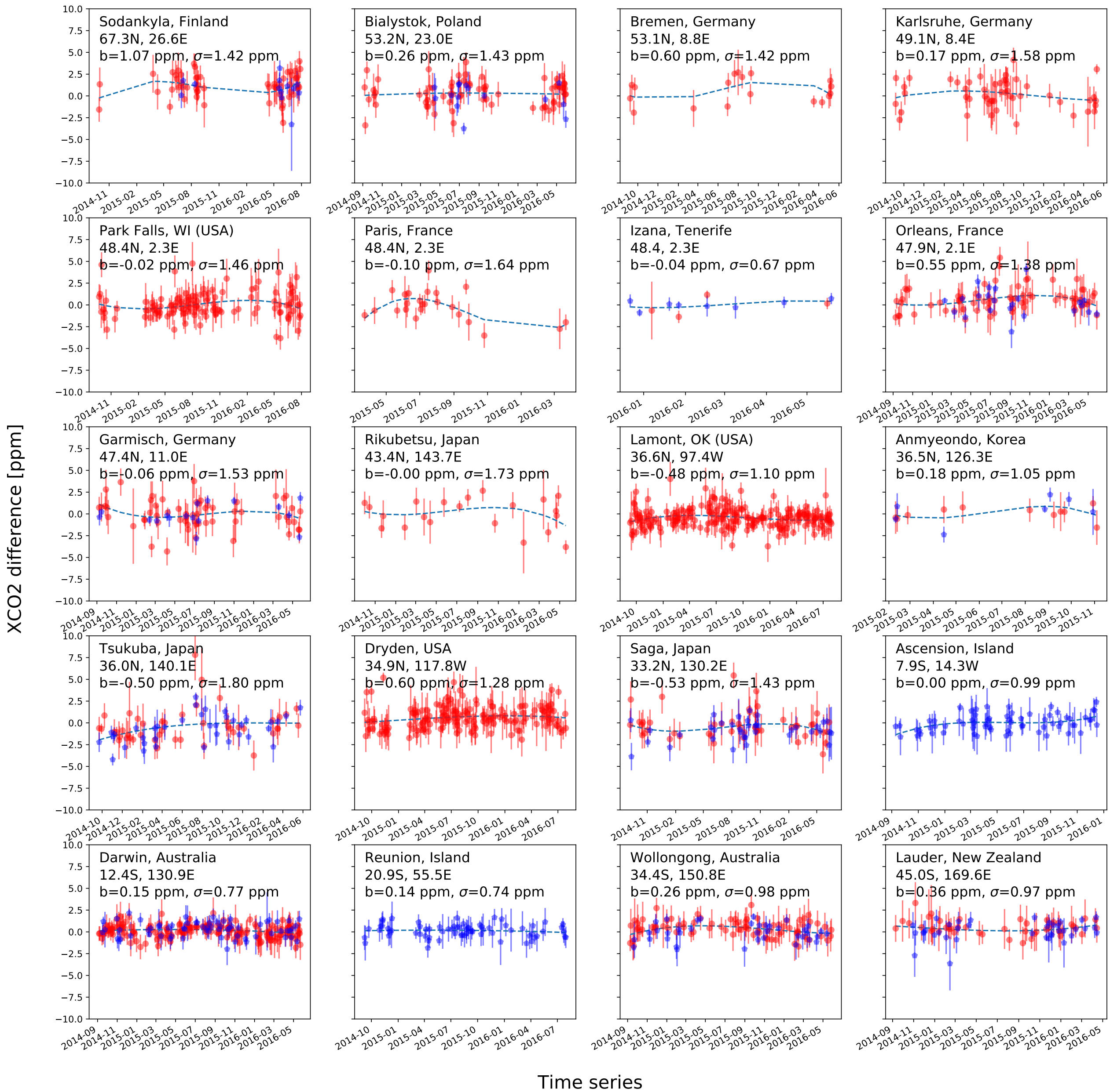

Figure 11. Time variation of X_{CO_2} difference between retrievals from OCO-2 observations over land (red dots) and ocean (blue pentagon) and collocated TCCON measurements for each TCCON station. Standard deviation of individual TCCON measurement and satellite retrievals are presented with the length of bar. In each subplot, the overall bias (b), standard deviation(σ) and site location in latitude and longitude are included. The shown results here are bias-corrected data used in Table 3. An second order polynomial (blue dot lines) is fitted for distinguishing the time-variation of biases.

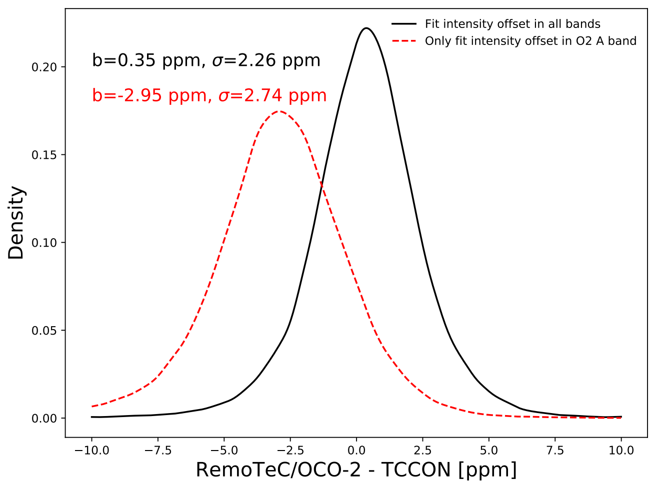

Figure 12. Density distributions of the X_{CO_2} differences between OCO-2 land retrievals and collocated TCCON data for two different retrieval settings. In the black solid line we fit intensity offsets in all three OCO-2 bands while in the red dashed line we only fit the intensity offset in O_2A band. Here we only do algorithm convergence filtering for both and take the intersection of them for fair comparison. The bias b and sounding precision σ for each retrieval are included.

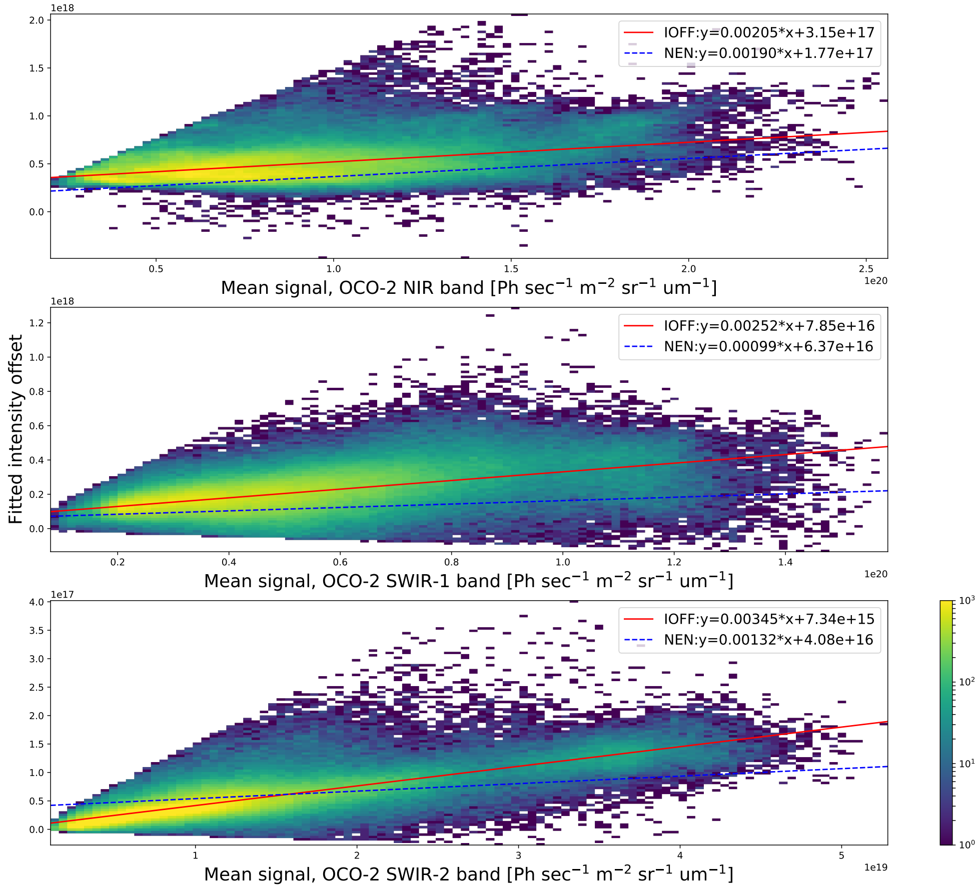

Figure 13. Variation of fitted intensity offset with respect to mean signals measured in each OCO-2 band for observations over land. Linear regression fit for the intensity offset (IOFF) and noise equivalent radiance (NEN) is overplotted along with fitted cofficients on top right. Different colors represent the frequency of point occurrence.